CRYOGENIC-PROPELLANT HEATING IN THE THERMAL ENVIRONMENT OF SPACE

By G. R. Smolak and R. H. Knoll

Lewis Research Center
National Aeronautics and Space Administration
Cleveland, Ohio

Presented at the
Conference On Aerodynamically Heated Structures

Sponsored by
Office of Scientific Research
Arthur D. Little, Inc.

July 25, 26, 1961
Cambridge, Massachusetts

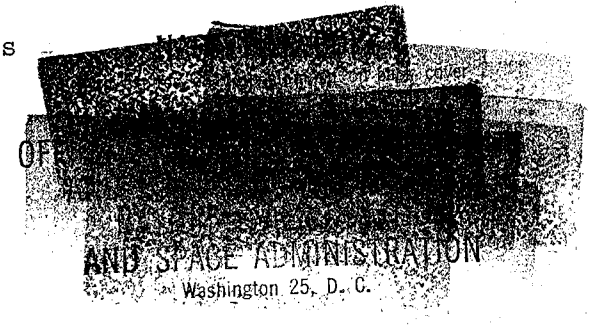

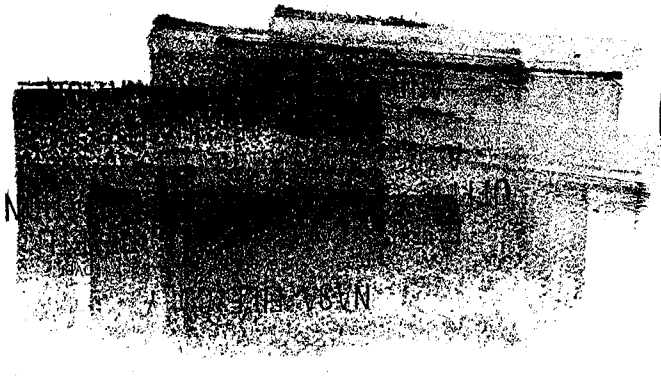

CRYOGENIC-PROPELLANT HEATING IN THE THERMAL ENVIRONMENT OF SPACE

By G. R. Smolak and R. H. Knoll

Lewis Research Center
National Aeronautics and Space Administration
Cleveland, Ohio

ABSTRACT

Heat is transferred to a propellant tank in space from the Sun, planets, and on-board components. Radiation and conduction from adjacent components are relatively simple to define and are a familiar problem to the designer of Dewars for ground installations. Unless heat transfer to cryogenic propellants from these on-board sources is extremely small, there will be excessive propellant vaporization. The heat transfer by radiation from the Sun and planets to propellant tanks is discussed in detail as is the effect of using various thermal barriers to reduce propellant heating. An extensive list of equations is included to summarize the results of the analytical derivations for each particular thermal-protection system.

Operation in a planet orbit, in general, subjects the propellants to a time-varying radiation environment. The attitude of the tank with respect to both the Sun and a nearby planet must be known at all times in order to estimate propellant heating rates accurately. The choice of orbit altitude provides some possibility for alleviation of adverse propellant heating effects.

Of major concern in the preliminary analysis of a space vehicle is the maximization of payload weight. The ultimate effect of the thermal environment of space on the design of a particular vehicle is a weight

penalty directly chargeable to this environment. A method of calculating and optimizing this weight penalty is included for a hypothetical Mars trip with a hydrogen-oxygen-fueled chemical stage.

CRYOGENIC-PROPELLANT HEATING IN THE THERMAL ENVIRONMENT OF SPACE

By G. R. Smolak and R. H. Knoll

Lewis Research Center
National Aeronautics and Space Administration
Cleveland, Ohio

INTRODUCTION

Cryogenic (low-temperature) liquids are among the best propellants currently available for both chemical- and nuclear-rocket stages. At present, the highest specific impulses for chemical rockets are obtained by using hydrogen and oxygen or hydrogen and fluorine as propellants. Many proposed nuclear-rocket propulsion systems utilize hydrogen as the working fluid.

During the course of an interplanetary space mission, heat transfer to these cryogenic liquids from the Sun, planets, planet atmospheres, and from other components of the rocket vehicle is inevitable. This heating causes propellant vaporization and consequent loss by venting. Unless these losses are small, the potential advantage of using cryogenic propellants would be negated. Thus, thermal protection of the cryogenic liquids from the adverse heating environment is required.

Aerodynamic heating of propellants during boost has been discussed in references 1 and 2. The storage of propellants in circular satellite orbits has been treated in references 3 and 4. References 5 and 6 have examined the problem of propellant storage in the space environment away from planets. An analysis of hydrogen storage problems for a nuclear-rocket mission to Mars or Venus was made in reference 7. The thermal-protection systems considered were reflective shields, attitude control,

refrigeration, and freezing. The problem of cryogenic-propellant boiloff for hypothetical Mars and Venus trips using hydrogen and oxygen propellants has been analyzed in reference 8. The methods of reference 8 were used in reference 9 to account for the thermal-protection systems required on manned nuclear-rocket missions to Mars.

The objectives of this paper are to examine the problem of heat absorption by cryogenic propellants due to the thermal-radiation environment of space and to compare the effectiveness of various thermal-protection devices for specific applications.

This paper provides the basic methods of analysis required to predict the heat-transfer rates through various thermal-protection devices. These methods can be used to design a thermal-protection system for a particular application. Several methods of reducing propellant heating are discussed in this paper. These are: spacing between components of the vehicle, thermal-radiation shielding, orientation of the vehicle with respect to the Sun, and coatings. The effectiveness of these thermal-protection methods are compared for reducing both on-board heating and external heating from the Sun and planets. To illustrate the procedure for choosing a particular thermal-protection system, the design of such systems for a hypothetical hydrogen-oxygen chemical-rocket terminal stage for a Mars mission is presented.

The material presented in this paper will be amplified in reference 10, which is currently in the publication process.

ANALYSIS

The sources of propellant heating may be either internal or external with respect to the rocket vehicle. Several methods of protection against these heat fluxes will be discussed.

HEAT SOURCES

ON-BOARD SOURCES. - Propellant tanks will be subjected to thermal radiation and conduction from adjacent components of the vehicle and to nuclear-heating effects from the nuclear reactor if one is used for propulsion or auxiliary power. Heating caused by the gamma rays and neutron flux of a reactor has been investigated in references 11 and 12. Therefore, no treatment of nuclear-heating effects will be made herein.

Heating of cryogenic propellants due to adjacent components is caused by thermal radiation, and by conduction through propellant lines and structural members. The rate of heating by radiation is approximately proportional to the difference between the fourth powers of the absolute temperatures of the adjacent component and the propellant. This can become relatively large if a low-temperature cryogenic is near a high-temperature (about room temperature or warmer) component. The rate of heat transfer per unit area by conduction is directly proportional to the product of temperature difference between adjacent components and thermal conductivity of the conductor and inversely proportional to the length of the heat path.

The structural members which separate and support propellant tanks must be designed so as to ensure low rates of heat conduction. In reference 11 this was done by using low-conductivity laminated stainless-steel supports as suggested in reference 13.

The heat transfer to propellants by conduction through propellant lines need not be a major problem. One solution might be to use self-sealing quick-disconnect couplings in appropriate propellant lines.

EXTERNAL SOURCES. - The external sources of heat are the Sun and the planets. Heat is transferred between these sources and the cryogenic storage system by thermal radiation. The largest external heat flux encountered by a vehicle within our solar system is that which originates from the Sun. For a unit area that is perpendicular to a radius vector from the Sun, this flux (outside of planet atmospheres) is inversely proportional to the square of the distance from the Sun, and is given by

$$\left(\frac{\dot{Q}}{A}\right)_S = \frac{428}{S^2}, \frac{\text{Btu}}{(\text{hr})(\text{sq ft})} \tag{1}$$

(See appendix for the definition of all symbols.)

The heat flux that a vehicle receives from a planet results partly from planetary radiation and partly from reflected solar radiation. This planetary heat flux is given by

$$\frac{\dot{Q}}{A} = f\left(\sigma\epsilon_P T_P^4 + \frac{428 a_P z}{S^2}\right) \tag{2}$$

The planetary heat flux increases as the distance from a planet decreases and can be of the same order of magnitude as the solar flux. Although this planetary flux becomes relatively large, it never exceeds the solar flux.

ASSUMPTIONS

As a simplification, it was assumed in many examples herein that a typical space vehicle is composed of components (payload, fuel, and

perhaps an oxidant) having circular cross-sectional areas and arranged on a common axis. Several additional assumptions were:

(a) The vehicle components are at a constant temperature and steady-state conditions prevail.

(b) The effective temperature of space is equal to 0° R except where noted.

(c) Absorptivities and emissivities are total hemispherical values.

(d) Radiation leaving a surface (including reflected radiation) is diffuse.

(e) Shadow shields and foils are parallel, thermally isolated, reflective surfaces and have the same temperature on both faces.

METHODS OF REDUCING PROPELLANT HEAT ABSORPTION DUE TO ON-BOARD SOURCES

A summary of the heat-transfer relations for propellant tanks with various thermal-protection systems and in various extra-atmospheric thermal environments is shown in table I.

SPACING OF COMPONENTS. - From the equations for model 1 in table I, it is apparent that the heat flux from on-board sources can be decreased by increasing the distance between components. However, when propellants are subjected to radiation from external sources as well as on-board heat flux, increasing the distance between components may not be desirable.

REFLECTIVE SHIELDS. - The heat transfer between adjacent components can be greatly reduced by interposing parallel, thermally isolated, reflective shields. Models 2 and 3 in table I list the equations for heat-absorption rates in such a circumstance. Throughout this

TABLE I. - HEAT-TRANSFER RELATIONS FOR PROPELLANT TANKS WITH VARIOUS THERMAL-PROTECTION SYSTEMS AND *IN VARIOUS EXTRA-ATMOSPHERIC THERMAL ENVIRONMENTS*

Model number	Model	Comments	Equations
1	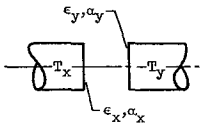	(a) Adjacent flat-ended cylindrical tanks	(a) $\left(\frac{Q}{A}\right)_y = \frac{\sigma\epsilon_x f_{x,y}\alpha_y T_x^4}{1-f_{x,y}f_{y,x}(1-\alpha_x)(1-\alpha_y)} + \frac{\sigma\epsilon_y f_{x,y}f_{y,x}(1-\alpha_x)\alpha_y T_y^4}{1-f_{x,y}f_{y,x}(1-\alpha_x)(1-\alpha_y)} - \sigma\epsilon_y T_y^4$
		(b) $\epsilon_x = \epsilon_y = \alpha_x = \alpha_y = \epsilon$ and $f_{x,y} = f_{y,x} = f$	(b) $\left(\frac{Q}{A}\right)_y = \frac{\sigma\epsilon^2 f T_x^4}{1-f^2(1-\epsilon)^2} + \frac{\sigma\epsilon^2 f^2(1-\epsilon)T_y^4}{1-f^2(1-\epsilon)^2} - \sigma\epsilon T_y^4$
		(c) $f_{x,y} = f_{y,x} \approx 0$ (i.e., large distances between x and y)	(c) $\left(\frac{Q}{A}\right)_y = -\sigma\epsilon_y T_y^4$
		(d) $f_{x,y} = f_{y,x} \approx 1$ (i.e., x and y are very close together)	(d) $\left(\frac{Q}{A}\right)_y = \frac{\sigma(T_x^4 - T_y^4)}{\frac{1}{\epsilon_y} + \frac{1}{\epsilon_x} - 1}$
2	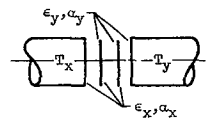	(a) One shadow shield between x and y. $f_{x,y} = f_{y,x} = f$	(a) $\left(\frac{Q}{A}\right)_y = \frac{\sigma(\epsilon_x^2\alpha_y^2 f^2 T_x^4 + \alpha_y\alpha_x\epsilon_y\epsilon_x T_y^4)}{[1-f^2(1-\alpha_y)(1-\alpha_x)][\epsilon_y(1+\alpha_x f^2 - f^2) + \epsilon_x(1-\alpha_y f^2 - f^2)]} - \frac{\sigma\epsilon_y(1+\alpha_x f^2 - f^2)T_y^4}{[1-f^2(1-\alpha_y)(1-\alpha_x)]}$
		(b) One shadow shield $f_{x,y} = f_{y,x} = 1$	(b) $\left(\frac{Q}{A}\right)_y = \frac{\sigma\epsilon_y[(\alpha/\epsilon)_y(\epsilon/\alpha)_x]^{N+1}T_x^4 - \sigma\epsilon_y T_y^4}{\left(1-\alpha_y+\frac{\alpha_y}{\alpha_x}\right)\left\{\frac{1-[(\alpha/\epsilon)_y(\epsilon/\alpha)_x]^{(N+1)}}{1-[(\alpha/\epsilon)_y(\epsilon/\alpha)_x]}\right\}}$
		(c) One shadow shield $\alpha_x = \epsilon_x$ and $\alpha_y = \epsilon_y$	(c) $\left(\frac{Q}{A}\right)_y = \frac{\sigma(T_x^4 - T_y^4)}{\left(\frac{1}{\epsilon_y} + \frac{1}{\epsilon_x} - 1\right)(N+1)}$
		(d) Two shadow shields	(d) See ref. 10 (equations too lengthy for tabulation here)
		(e) N equally spaced shadow shields where $N > 2$	(e) See ref. 10 (equations too lengthy for tabulation here)
		(f) N foils between tanks	(f) $\left(\frac{Q}{A}\right)_y = \frac{\sigma\epsilon_y[(\alpha/\epsilon)_y(\epsilon/\alpha)_x]^{(N+1)}T_x^4 - \sigma\epsilon_y T_y^4}{\left(1-\alpha_y+\frac{\alpha_y}{\alpha_x}\right)\left\{\frac{1-[(\alpha/\epsilon)_y(\epsilon/\alpha)_x]^{N+1}}{1-[(\alpha/\epsilon)_y(\epsilon/\alpha)_x]}\right\}}$
		(g) N foils between tanks $\alpha_x = \epsilon_x$, $\alpha_y = \epsilon_y$	(g) $\left(\frac{Q}{A}\right)_y = \frac{\sigma\epsilon_y(T_x^4 - T_y^4)}{\left(1-\epsilon_y+\frac{\epsilon_y}{\epsilon_x}\right)(N+1)}$

TABLE I. - Continued. HEAT-TRANSFER RELATIONS FOR PROPELLANT TANKS WITH VARIOUS THERMAL-PROTECTION SYSTEMS AND IN VARIOUS EXTRA-ATMOSPHERIC THERMAL ENVIRONMENTS

Model number	Model	Comments	Equations
3	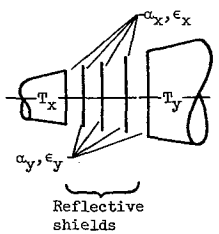	(a) One shadow shield between tanks - all arranged in conical envelope. Angle factors between adjacent surfaces are constant going in one direction (i.e., $f_{y,1} = f_{1,x}$)	(a) $\left(\frac{\dot{Q}}{A}\right)_y = \frac{\left[\frac{\sigma\epsilon_x f_{1,y}\alpha_y}{1 - f_{1,y}f_{y,1}(1-\alpha_x)(1-\alpha_y)}\right]^2 \frac{A_x}{A_y} T_x^4 + \frac{\sigma^2\epsilon_y f_{y,1}\alpha_x\epsilon_x f_{1,y}\alpha_y}{[1 - f_{1,y}f_{y,1}(1-\alpha_x)(1-\alpha_y)]^2} T_y^4}{\left\{\sigma(\epsilon_y + \epsilon_x) - \frac{[\sigma\epsilon_x f_{1,y}f_{y,1}(1-\alpha_y)\alpha_x + \sigma\epsilon_y f_{1,y}f_{y,1}(1-\alpha_x)\alpha_y]}{1 - f_{y,1}f_{1,y}(1-\alpha_x)(1-\alpha_y)}\right\}}$ $+ \left[\frac{\sigma\epsilon_y f_{1,y}f_{y,1}(1-\alpha_x)\alpha_y}{1 - f_{1,y}f_{y,1}(1-\alpha_x)(1-\alpha_y)} - \sigma\epsilon_y\right] T_y^4$
		(b) Two or more shadow shields. Angle factors between surfaces are constant going in one direction	(b) See ref. 10 (equations too lengthy for tabulation here).
4	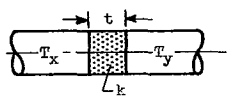	Insulation between tanks	$\left(\frac{\dot{Q}}{A}\right)_y = \frac{k}{t}(T_x - T_y)$
5	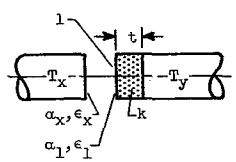	Insulation on tank y. Gap between insulation and tank x	Solution by trial-and-error method is given in ref. 10.
6	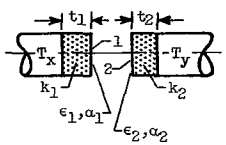	Insulation on both tanks. Gap between tanks	
7	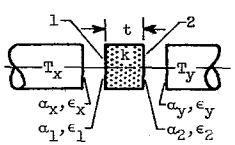	Insulation between tanks but not attached to either tank. Angle factors between x and 1 and between y and 2 are equivalent	

TABLE I. - Continued. HEAT-TRANSFER RELATIONS FOR PROPELLANT TANKS WITH VARIOUS THERMAL-PROTECTION SYSTEMS AND IN VARIOUS EXTRA-ATMOSPHERIC THERMAL ENVIRONMENTS

Model number	Model	Comments	Equations
8	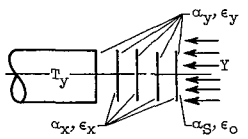 Reflective shields equally spaced	(a) One shadow shield	(a) $\left(\frac{\dot{Q}}{A}\right)_y = \frac{\alpha_S \epsilon_x \alpha_y f Y}{[1 - f^2(1-\alpha_x)(1-\alpha_y)](\epsilon_o + \epsilon_x) - \epsilon_x f^2(1-\alpha_y)\alpha_x} + \frac{\sigma\epsilon_y f^2(1-\alpha_x)\alpha_y T_y^4}{[1 - f^2(1-\alpha_y)(1-\alpha_x)]} - \sigma\epsilon_y T_y^4 + \frac{\sigma\alpha_y\alpha_x\epsilon_y\epsilon_x f^2 T_y^4}{[1 - f^2(1-\alpha_y)(1-\alpha_x)]\left\{[1 - f^2(1-\alpha_y)(1-\alpha_x)](\epsilon_o + \epsilon_x) - \epsilon_x f^2(1-\alpha_y)\alpha_x\right\}}$
		(b) Two or more shadow shields	(b) See ref. 10 (equations too lengthy for tabulation here).
		(c) One or more foils	(c) $\left(\frac{\dot{Q}}{A}\right)_y = \frac{(\alpha_S/\epsilon_o)[(\alpha/\epsilon)_y(\epsilon/\alpha)_x]^N \epsilon_y Y - \sigma\epsilon_y T_y^4}{\left(1 - \alpha_y + \frac{\alpha_y}{\alpha_x}\right)\left\{\frac{1 - [(\alpha/\epsilon)_y(\epsilon/\alpha)_x]^N}{1 - [(\alpha/\epsilon)_y(\epsilon/\alpha)_x]} + \frac{\epsilon_y}{\epsilon_o}\left[\left(\frac{\alpha}{\epsilon}\right)_y\left(\frac{\epsilon}{\alpha}\right)_x\right]^N\right\}}$
		(d) One or more foils $\alpha_x = \epsilon_x$, $\alpha_y = \epsilon_y$	(d) $\left(\frac{\dot{Q}}{A}\right)_y = \frac{\alpha_S Y - \sigma\epsilon_o T_y^4}{\epsilon_o\left(\frac{1}{\epsilon_y} + \frac{1}{\epsilon_x} - 1\right)N + 1}$
9	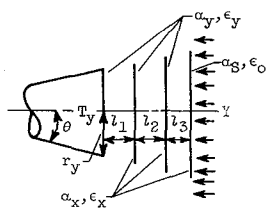 Reflective shields	(a) One shadow shield on the end of a tank. All elements form a conical envelope.	(a) $\left(\frac{\dot{Q}}{A}\right)_y = \frac{\frac{\sigma\epsilon_x f_{1,y}\alpha_y\alpha_S Y\left(1 + \frac{l_1}{r_y}\tan\theta\right)^2}{1 - f_{1,y}f_{y,1}(1-\alpha_x)(1-\alpha_y)} + \frac{\sigma^2\epsilon_y f_{y,1}\alpha_x\epsilon_x f_{1,y}\alpha_y T_y^4}{[1 - f_{1,y}f_{y,1}(1-\alpha_x)(1-\alpha_y)]^2}}{\sigma(\epsilon_o + \epsilon_x) + \frac{\sigma\epsilon_x f_{1,y}f_{y,1}(1-\alpha_y)\alpha_x}{1 - f_{1,y}f_{y,1}(1-\alpha_x)(1-\alpha_y)}} + \left[\frac{\sigma\epsilon_y f_{1,y}f_{y,1}(1-\alpha_x)\alpha_y}{1 - f_{1,y}f_{y,1}(1-\alpha_x)(1-\alpha_y)} - \sigma\epsilon_y\right]T_y^4$
		(b) Two or more shadow shields arranged in conical envelope. All angle factors equal going in one direction (i.e., $f_{y,1} = f_{1,2} = f_{2,3} = \cdots$ and $\cdots = f_{3,2} = f_{2,1} = f_{1,y}$).	(b) See ref. 10 (equations too lengthy for tabulation here).

TABLE I. - Concluded. HEAT-TRANSFER RELATIONS FOR PROPELLANT TANKS WITH VARIOUS THERMAL-PROTECTION SYSTEMS AND IN VARIOUS EXTRA-ATMOSPHERIC THERMAL ENVIRONMENTS

Model number	Model	Comments	Equations
10	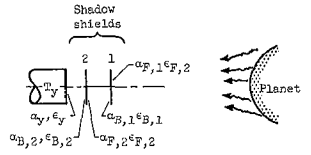	Two shadow shields equally spaced. Equal angle factors between shields. Shields same diameter as tank. Angle factor between shield and space equals one (1) minus angle factor between shields. Temperature of space can be other than 0° R. Portion of shield which cannot "see" planet is at different temperature than portion of same shield which "sees" planet. No conduction of heat between these two areas on same shield. Surface y may be covered with layer of insulation having thickness t and thermal conductivity k or with N foils - all surfaces of which have $\alpha = \epsilon = \alpha_y$.	See ref. 10 (equations too lengthy for tabulation here). When insulation or foils are on surface y, a rapidly convergent trial-and-error solution can be used.
11	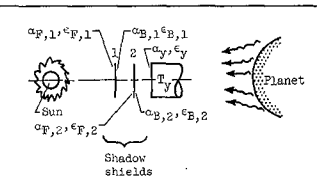		
12	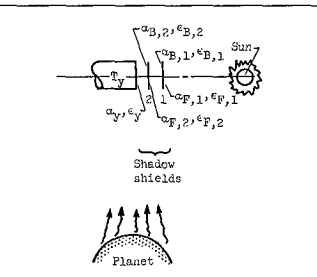	Two shadow shields in plane perpendicular to line passing through center of Sun and planet (sketch exaggerated). Planetary flux reflected only once before passing into space. Surface y may be covered with insulation or foils as in models 10 and 11 above. Temperature of space may be other than 0° R.	
13	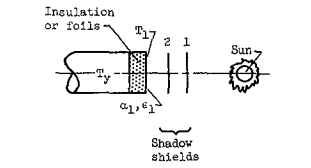	Two shadow shields. Insulation or foils immediately adjacent to tank. The same as case 8(b) in other respects	
14	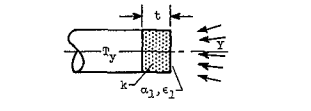	Tank surface covered with insulation	See ref. 10. Trial-and-error solution required.
15	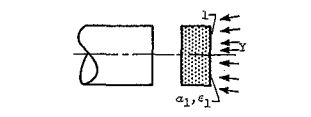	Y incident only on surface 1. Heat transfer only axially through insulation.	

this paper, the term "foil" is used when the angle factor between adjacent surfaces is equal to unity. The term "shadow shield" is used when the angle factor between adjacent surfaces is less than unity.

INSULATION. - Another means of reducing the heat transfer between components is to use insulation. The equation resulting when a purely insulative material is inserted between propellant tanks is shown with model 4 in table I. Models 5, 6, and 7 are included to indicate possible combinations of insulation materials with spacing between components.

METHODS OF REDUCING PROPELLANT HEAT ABSORPTION DUE TO EXTERNAL SOURCES

The methods of reducing heat absorption due to external sources, which will be discussed are: coatings having a low absorptivity for the incident radiation, reflective surfaces, and proper orientation of the propellant tank with respect to the incident radiation.

COATINGS. - If it is assumed, as shown in sketch (a), that flux Y is incident upon an element of surface area A having an absorptivity

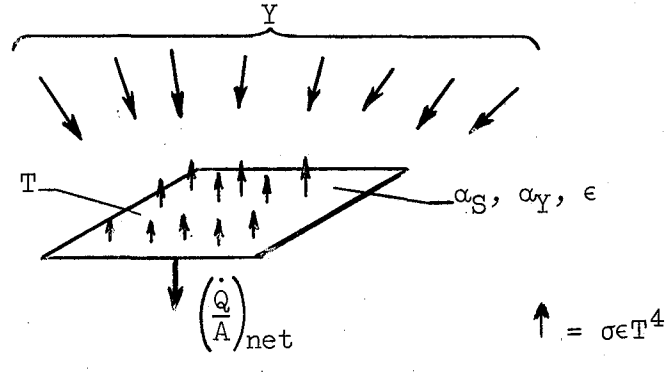

(a)

for flux Y of α_Y, an emissivity of ϵ, and a temperature T, then the net rate of heat transfer through the surface is, in general

$$\left(\frac{\dot{Q}}{A}\right)_{net} = \alpha_Y Y - \sigma\epsilon T^4 \qquad (3)$$

For the special case where Y is direct or reflected solar flux, $\alpha_Y = \alpha_S$, and equation (3) becomes

$$\left(\frac{\dot{Q}}{A}\right)_{net} = \alpha_S Y - \sigma\epsilon T^4 \qquad (4)$$

In general, if Y is from a body at a temperature less than the melting point of common metals, then $\alpha_Y = \epsilon$. If Y is from the Sun, $\alpha_Y = \alpha_S \neq \epsilon$. Then α_S/ϵ may be less than or greater than unity depending on the composition of surface A. For problems involving storage of propellants near the Earth, $Y_{maximum}$ is about 428 Btu/(hr)(sq ft). In order to minimize $(\dot{Q}/A)_{net}$, a material or coating having low α_S and high ϵ should be used. For silica oxide on magnesium, reference 14 gives $\alpha_S = 0.21$ and $\epsilon = 0.83$. Therefore, in order for the T^4 term to be significant (say 1 percent as large as the Y term), T must be greater than about 160° R. Thus, coatings for bare cryogenic tanks should have mainly low values of α_S. Coatings for higher-temperature surfaces (where the energy emitted by the surface is nearly as large as the energy absorbed) should have not only a low value of α_S but also a high value for ϵ.

The rate of heat absorption by a surface in space subjected to solar flux is obviously strongly dependent upon the values of solar absorptivity and emissivity peculiar to the surface. Some control of these properties is possible through the use of coatings (paints, oxides, metals, etc.).

Emissivity values may range from 0.02 to about 0.9, and solar absorptivity to emissivity ratios may range from about 0.2 to 21 (refs. 14 to 16). However, as shown in reference 15, the solar absorptivity and emissivity may change significantly because of ascent heating, Van Allen radiation, sputtering, meteoroid erosion, the ultraviolet component of solar radiation, and prelaunch oxidation and corrosion. Consequently, conservative assumptions for surface properties have been assumed herein. To suggest at this time using extremely low values for α_s or ϵ for lengthy space missions would involve considerable risk of change in these surface properties during the mission.

For most space missions there would undoubtedly be an optimum coating or material to use for each particular surface of a vehicle. To indicate such optimums is beyond the scope of this paper.

REFLECTIVE SHIELDS. - One method of reducing the heat transfer into an exposed cryogenic-tank surface is to place shadow shields between the cryogenic surface and the external heat source, as shown by model 8 in table I. When the incoming waves of radiation are incident only on the outer surface of the outermost shield, the expression for the net rate of heat absorption by surface y with one shadow shield placed between it and the external flux Y is given in the table.

The heat-absorption rate of a cryogenic-tank surface exposed to an external flux can also be reduced by applying foils. This case is the same as the shadow-shield case, except that, with foils, the angle factor between adjacent surfaces has a value of 1. The relations for the net heat-absorption rate of surface y with N foils protecting it are given in models 8(c) and (d).

A possible conical arrangement of shadow shields is shown in model 9 of table I. The equations for two or more shadow shields are presented in reference 10. In general, the heat-absorption rate can be decreased by increasing the number of shadow shields.

If shadow shields are used for protection from external radiation in the vicinity of planets, the equations describing the rate of heat absorption increase complexity. Models 10, 11, and 12 in table I show possible arrangements of double shadow shields. The resultant, rather lengthy, equations are given in reference 10. In some cases it may be desirable to have insulation or foils on a tank surface and in addition have two shadow shields between the tank and the Sun. This arrangement is shown as model 13.

If insulation is the means of protection against solar flux, it can be applied directly to the tank surface (model 14, table I) or separated a finite distance from the tank (model 15).

ORIENTATION. - For any body in space, the amount of heat absorbed from solar or planetary flux depends on the area exposed to these radiant heat sources. The amount of solar heat absorbed can be minimized by minimizing the projected area exposed to the Sun. Thus, for the vehicles shown in figure 1, the incident solar flux will be minimized by alining the longitudinal axis of the stage with the position vector of the stage relative to the Sun. At the extremely great distances from the Sun of concern here, the solar flux is nearly parallel. Thus, the sides of the vehicle essentially will not "see" the Sun. For space-vehicle operation in the vicinity of either the Sun or a planet, the apparent flux is not parallel. Therefore, while vehicle orientation can

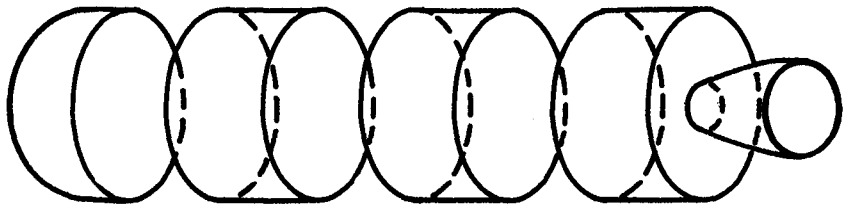

(a) TYPICAL CHEMICAL–ROCKET STAGE.

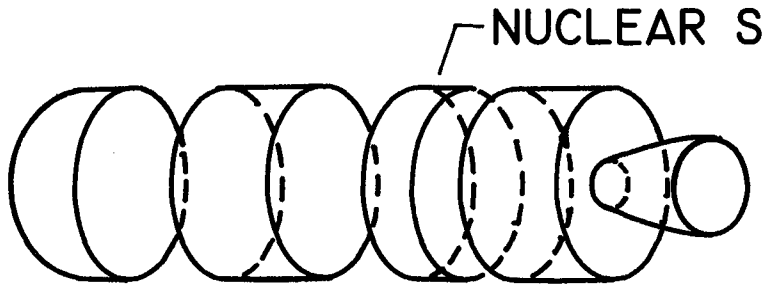

(b) TYPICAL NUCLEAR–ROCKET STAGE.

Figure 1. - Schematic diagrams of rocket stages.

minimize the projected area, it cannot completely eliminate the heating effect of this flux.

RESULTS AND DISCUSSION

Two space vehicles of current interest that use cryogenic propellants are: (1) the high-specific-impulse chemical rocket (with liquid hydrogen as the fuel and liquid oxygen or liquid fluorine as an oxidizer), and (2) the nuclear rocket (with liquid hydrogen as the fuel). Schematic diagrams of these vehicles are shown in figure 1. Each vehicle has a payload, one or more propellants, and an engine. It was assumed that the cross sections of the components were circular and that the propellant tanks were cylindrical. It was also assumed that the payload temperature was 520° R and that the propellants, hydrogen and oxygen, for example, were slightly subcooled, having constant temperatures of 30° and 140° R, respectively. With the basic components of these two vehicles defined, it is now possible to examine the various thermal-protection techniques suggested in the ANALYSIS.

THERMAL PROTECTION AGAINST ON-BOARD HEATING

INSULATION AND FOILS. - A comparison of the properties of insulation materials for use in reducing radiation between components is shown in figure 2. The parameter of comparison is the thermal conductivity times the density of the materials. For space-vehicle applications the material should be a good insulator and have a low density. Foam-type insulations have been widely used in ground installations at atmospheric pressure. However, the evacuated-powder-type insulations have a $k\rho$ factor of about one-tenth that of the foams. Finally, the multilayer radiation shielding materials have a $k\rho$ factor which is better than

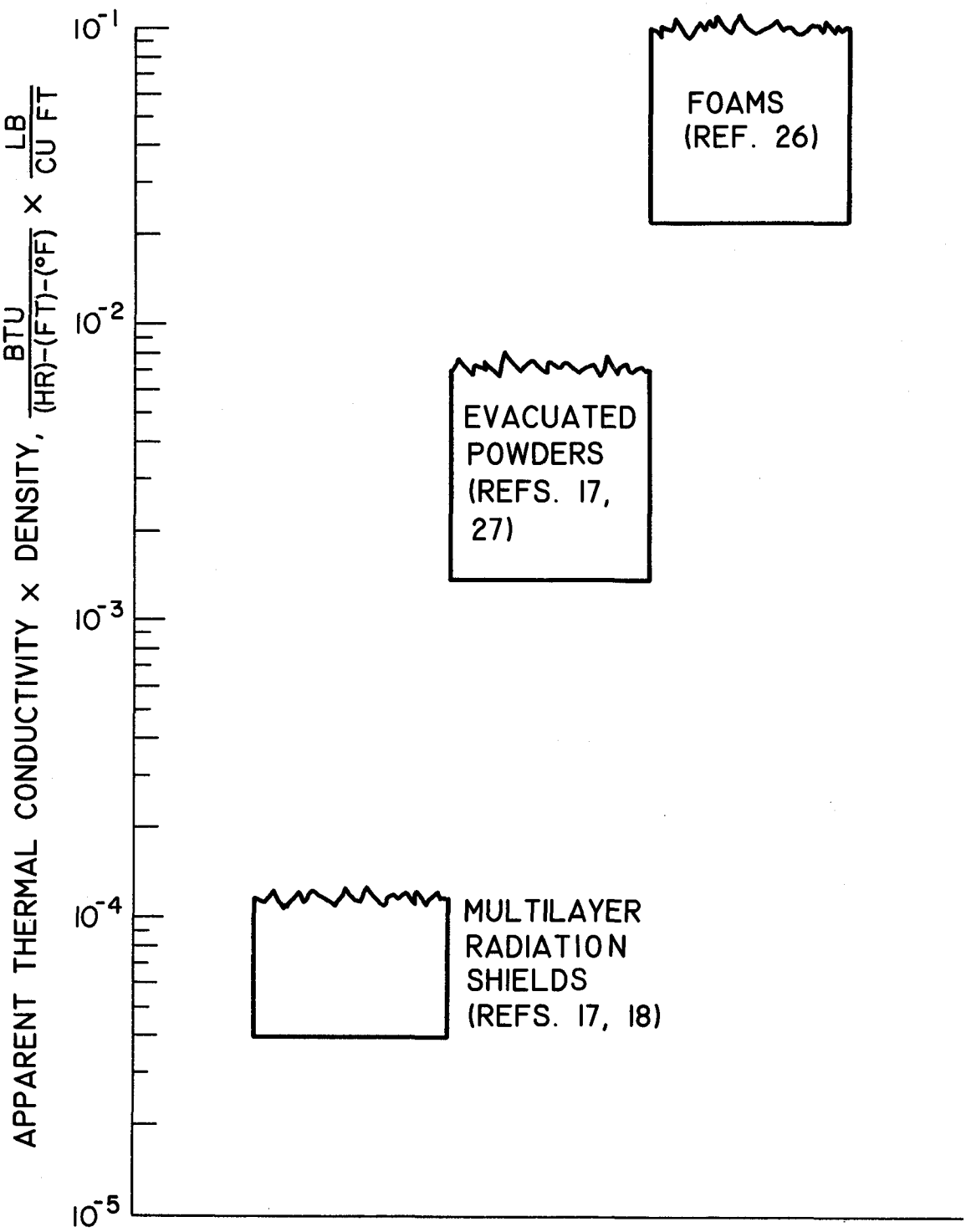

Figure 2. - Comparison of insulations for space applications.

the evacuated powders by a factor of about ten. Typical properties of these multilayer insulations are $k \approx 2.5 \times 10^{-5}$ Btu/(hr)(ft)($^{\circ}$F), $\rho = 4.7$ lb/cu ft, and 40 to 80 layers per inch. Thus, on a $k\rho$ basis, the multilayer radiation shields are clearly the most attractive materials for the thermal protection of cryogenic tanks in space. However, to ensure successful application of these materials, further experimental measurements should be made to obtain the properties of the multilayer shields when they are installed on propellant tanks. The effect of structural supports for such materials, and the effect of compressive loads on the thermal conductivity of the multilayer materials, should be determined. Compressive loads, which generally greatly increase the thermal conductivity, may be the result of either evacuation of the materials before launch or aerodynamic loading during the boost period.

In the analysis of thermal-protection systems it is convenient to express the thermal properties of the multilayer radiation shields by using radiation theory. With the radiation theory, the heat transfer between two bodies at constant temperatures T_1 and T_2 can be expressed as

$$\frac{\dot{Q}}{A} = \frac{\sigma\epsilon\left(T_1^4 - T_2^4\right)}{(2 - \epsilon)(N + 1)} \tag{5}$$

(assuming N thermally isolated radiation shields are spaced between T_1 and T_2 and that all angle factors are unity). This relation was derived in reference 8 and is also shown in figure 3. The simple conduction theory for the heat-transfer rate for the same situation (assuming that the radiation shields are replaced by a purely insulative material) is

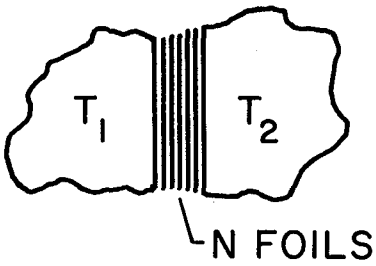

$T_1 > T_2$

$\alpha = \epsilon$

$$\left(\frac{\dot{Q}}{A}\right)_{CONDUCTION} = \frac{k}{t}(T_1 - T_2)$$

$$\left(\frac{\dot{Q}}{A}\right)_{RADIATION} = \frac{\sigma\epsilon(T_1^4 - T_2^4)}{(2-\epsilon)(N+1)}$$

IF $\left(\frac{\dot{Q}}{A}\right)_{CONDUCTION} = \left(\frac{\dot{Q}}{A}\right)_{RADIATION}$,

THEN

$$\epsilon_{EFFECTIVE} = \frac{2\left(\frac{k}{t}\right)(N+1)(T_1 - T_2)}{\sigma(T_1^4 - T_2^4) + \left(\frac{k}{t}\right)(N+1)(T_1 - T_2)}$$

$\epsilon_{effective}$	k, $\frac{Btu}{(hr)(ft)(^oF)}$	Thickness = 12t, in.	N	T_1, ^oR	T_2, ^oR	Reference
0.044-0.084	1.6×10^{-5}	0.5	20-40	540	138	18
0.064-0.093	2.5×10^{-5}	0.5	20-40	540	163	17
0.097	3×10^{-5}	1.5	75	540	137	19
0.097	2.4×10^{-5}	1.5	75	540	36	19
0.099	2.4×10^{-5}	1.5	75	535	36	19
0.099	2.3×10^{-5}	1.3	72	540	36	19

Figure 3. - Heat transfer between constant-temperature bodies.

$$\frac{\dot{Q}}{A} = \frac{k}{t}(T_1 - T_2) \tag{6}$$

By equating these relations and solving for ϵ and calling this value $\epsilon_{effective}$, we have

$$\epsilon_{effective} = \frac{2\left(\frac{k}{t}\right)(N + 1)(T_1 - T_2)}{\sigma\left(T_1^4 - T_2^4\right) + \frac{k}{t}(N + 1)(T_1 - T_2)} \tag{7}$$

Then, using published values (refs. 17 to 19) of k, t, N, T_1, and T_2, an effective emissivity corresponding to the commercial multilayer radiation-shield materials can be calculated. The results of such a calculation are shown in tabular form in the lower half of figure 3. All the materials shown have an effective value of emissivity of less than 0.1. Thus, the use of the radiation theory and assumptions of $\alpha = \epsilon = 0.1$ and 50 shields per inch conservatively approximates the performance of commercial multilayer radiation shielding materials. In addition, the temperature-dependence of thermal conductivity (rows 3 and 4 in fig. 3) is avoided. Absorptivities and emissivities on the order of 0.1 are typical of oxidized aluminum, polished stainless steel, and smooth unpolished Monel (refs. 13 and 20). Alternate layers of aluminum foil and submicron glass fiber paper compose a typical commercial foil insulation.

SHADOW SHIELDING. - Figure 4 demonstrates how shadow shields may be used to reduce on-board heat flux. In this figure the heat-absorption rate of hydrogen when placed adjacent to a 520° R source of heat is plotted against the number of shadow shields between the tanks. Several values of spacing ratio between adjacent surfaces are shown. For this figure and for several others throughout this paper, curves

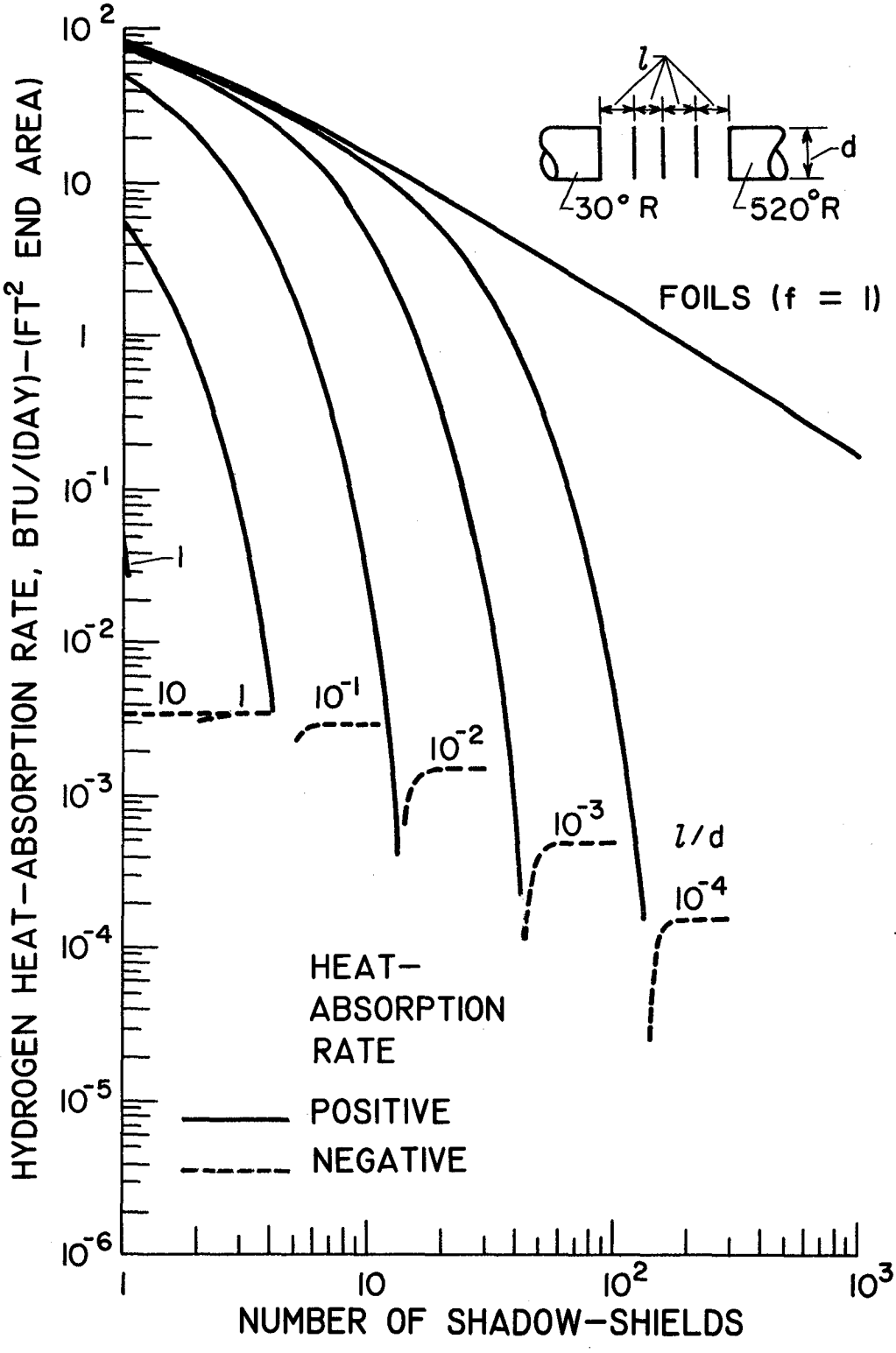

Figure 4. - Effect of number and spacing of shadow-shields on hydrogen heat-absorption rate due to on-board flux ($\alpha = \epsilon = 0.1$).

are shown even though data are valid only for integer values of reflective surfaces. Emissivity and absorptivity have been assumed equal to 0.1. From the figure it is apparent that shadow shields are capable of reducing the heat transfer between tanks considerably. For any given number of shadow shields, the heat-absorption rate decreases with increasing spacing ratio l/d. With extremely small l/d, the angle factor between adjacent shields approaches 1. Thus, the shadow-shield and foil equations should be expected to yield nearly the same value. Figure 4 shows this effect for small numbers of shields. For all l/d, if a large enough number of shadow shields is used, the hydrogen heat-absorption rate eventually becomes negative because of radiation to space from the shield and tank surfaces.

COMPARISON OF METHODS. - The choice of a particular method of achieving acceptable boiloff losses due to on-board heat flux between components is usually made on the basis of weight. Several elements of this weight problem are the weight of the protection device, the structural weight penalty necessary to employ the protection device, and the integrated weight of the propellant boiloff for the complete mission. The weight of individual shadow shields should be roughly the same as the weight of individual foils; however, additional structural support weight will be required to span the gap between shadow shields. Structural weights for these applications are greatly dependent on both size of the structure and the acceleration loads to which the structure will be subjected. These structures can vary from light inflatable structures to the heavy structures found between lower stages of multistage vehicles.

Thus, the structural weight problem must also be defined for each particular application before a final optimization of the thermal-protection system can be made.

THERMAL PROTECTION AGAINST SOLAR HEATING

Several methods for reducing the heating effect of solar flux will be discussed. These include using shadow shields, foils, and vehicle orientation with respect to the solar flux.

SHADOW SHIELDS. - The effect of the number and spacing of shadow shields on the heat-absorption rate of hydrogen due to solar flux at the Earth's distance from the Sun is shown in figure 5. The difference between figures 4 and 5 is that in figure 4 the temperature of the hottest surface is 520° R, while in figure 5 the temperature of the hottest surface varies with the number of shadow shields and the l/d between shields.

A possible shadow-shield structure would consist of rings supporting the edges of each shadow shield. Longitudinal members between components would support these rings and act as load-carrying members.

FOILS. - The effectiveness of using foils for protection against solar heating is shown in figure 6. The heat-absorption rate for a hydrogen-tank end surface exposed to solar radiation at the Earth's distance from the Sun is shown against the number of foils for constant values of emissivity. All the emissivities and absorptivities were assumed to be equal (i.e., $\alpha_S = \alpha = \epsilon$). The absorption rate can be decreased by either decreasing the foil emissivity or increasing the number of foils.

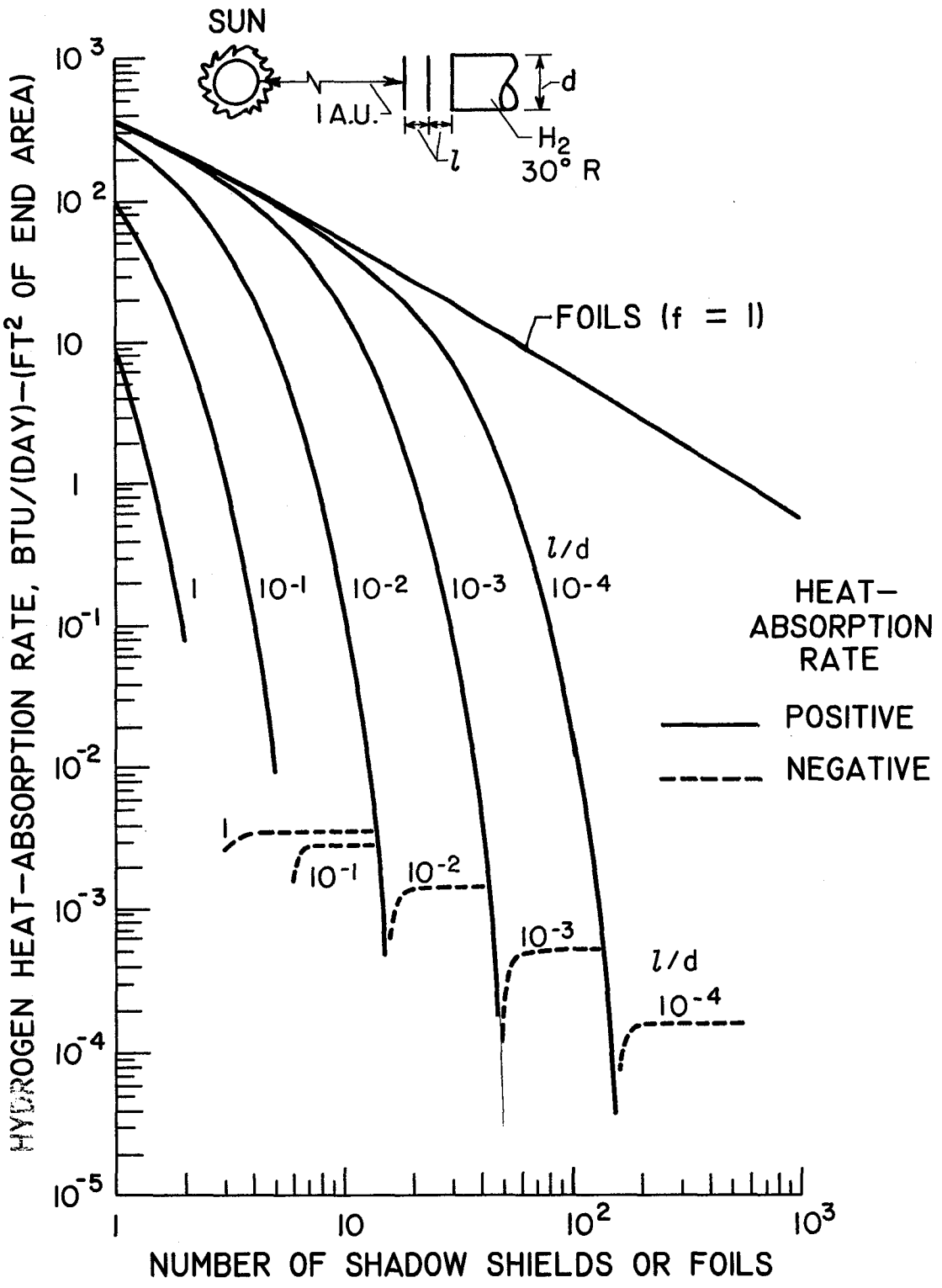

Figure 5. - Effect of number and spacing of shadow shields on hydrogen heat-absorption rate due to solar flux ($\alpha = \epsilon = 0.1$).

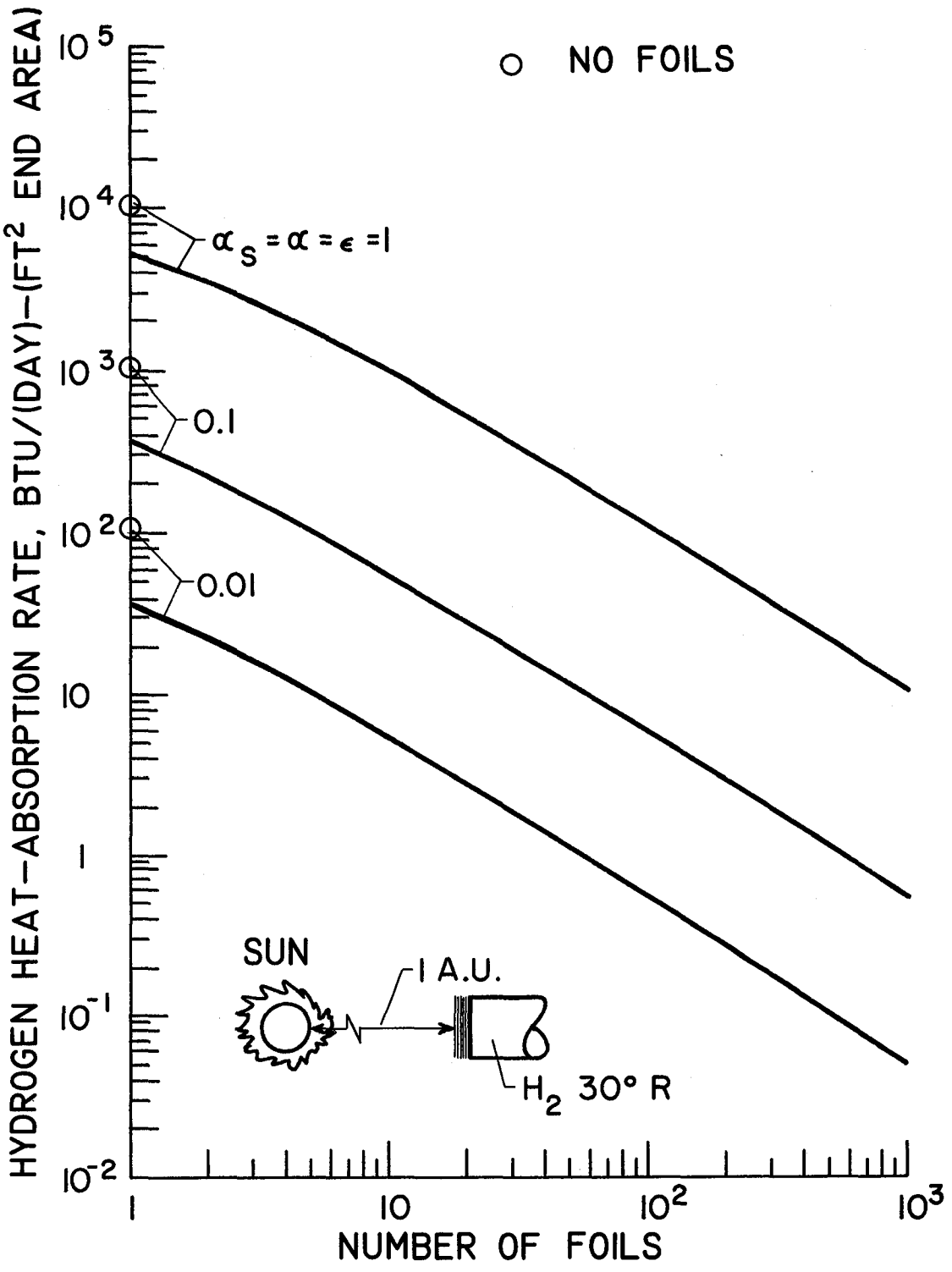

Figure 6. - Effect of number and emissivity of foils on hydrogen heat-absorption rate due to solar flux.

VEHICLE ORIENTATION. - One of the most obvious methods of protecting a cryogenic-tank surface from heating by solar radiation is to orient the stage so that one portion of the stage is used to cast a shadow on the cryogenic-tank surfaces. An attitude control system would be required to provide for proper orientation of the vehicle throughout the mission. However, an orientation system would probably be required anyway for such functions as attitude control of the vehicle prior to making propulsive maneuvers.

COMPARISON OF METHODS. - Figure 7 compares shadow shields and foils for protecting a hydrogen tank from direct solar radiation at the Earth's distance from the Sun assuming $\alpha = \epsilon = 0.1$. Hydrogen heat-absorption rate is plotted against the thickness occupied by the protection device. A specific tank diameter has been chosen for the shadow-shield data, because the absorption rate is dependent upon the angle factor between shields and the shield diameter. For a given thickness, ten shadow shields provide much lower absorption rates than one shadow shield. For thicknesses between 0.005 and 0.9 foot, the foils provide even lower absorption rates than the ten shadow shields. A weight comparison between the foils and shadow shields would again be difficult, because the weight optimization would involve the thermal-protection system, the structural weight penalty of this system, and the propellant boiloff.

THERMAL PROTECTION AGAINST PLANETARY HEATING

SHADOW SHIELDS. - Figure 8 shows a cylindrical cryogenic tank at low altitude above a planet surface with the longitudinal axis of the tank alined along the Sun-planet line. Radiation from the planet received

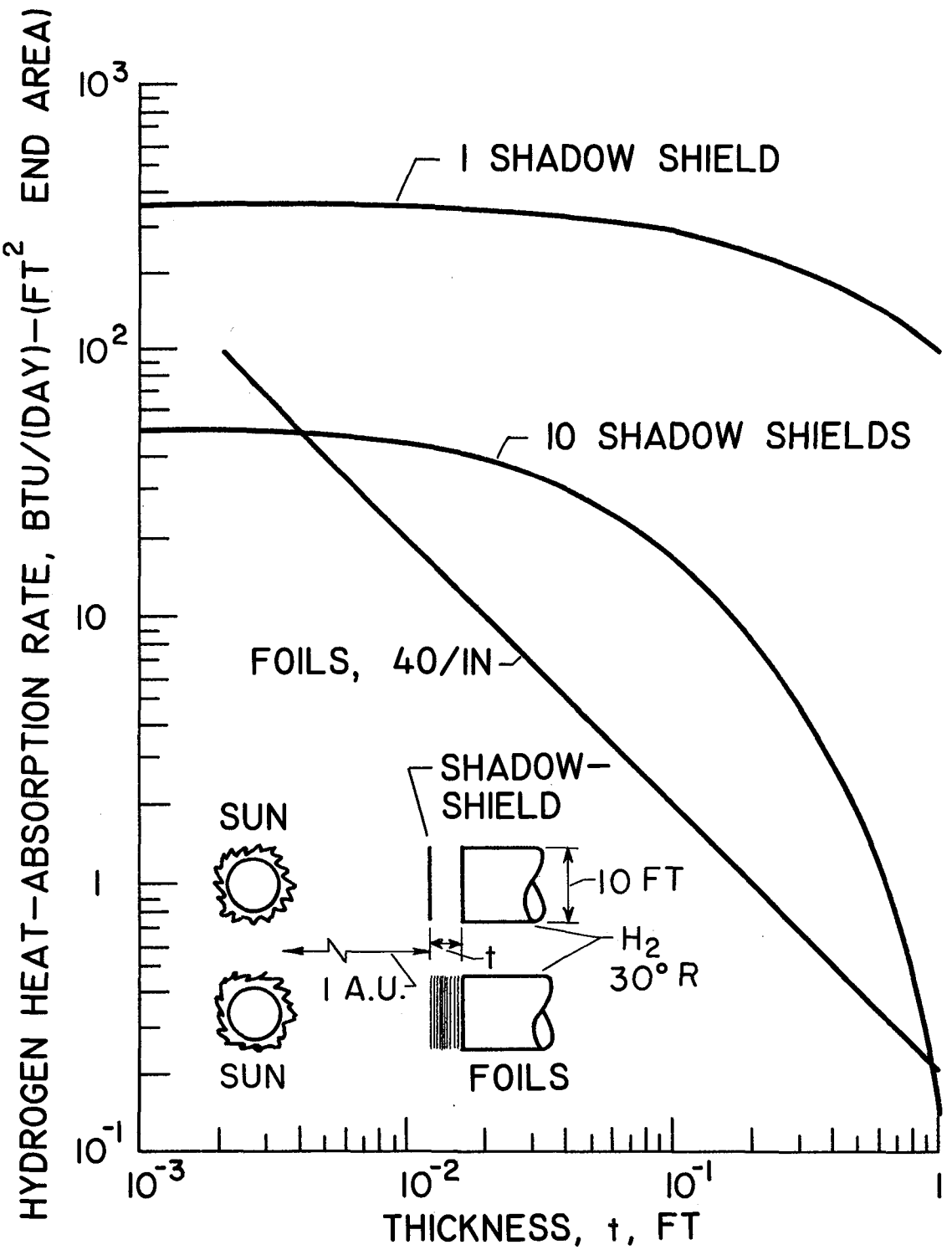

Figure 7. - Comparison of protection devices against solar heating on a thickness basis ($\alpha = \epsilon = 0.1$).

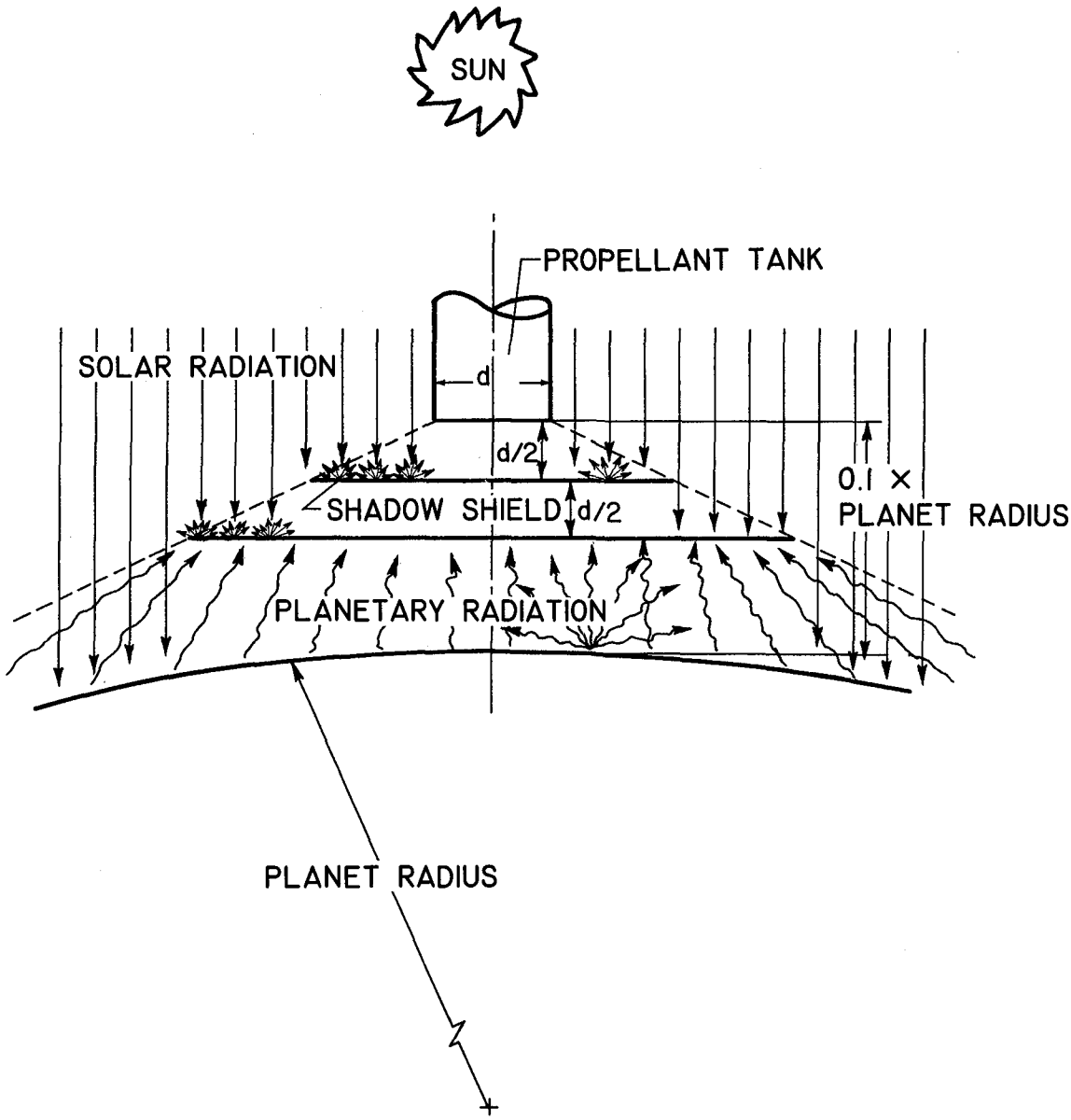

Figure 8. - Sketch showing effects of planetary and solar flux on planetary shadow shields.

by the tank end and side surfaces occupies a large solid angle. That is, the angle factors for planetary radiation are large at low altitudes. To intercept even the planetary radiation reaching the tank end with a single shadow shield or several shadow shields would require prohibitively large shields, as shown in the figure, unless the shields are placed very close to the end of the tank. In order to shadow a locally horizontal tank surface completely from planetary radiation, the shadow shields must occupy the same solid angle as the planet. The solid angle occupied by a planet increases as the distance from the planet decreases and approaches 2π steradians at the planet surface. Thus, the size of the shadow shield would become prohibitive at low-altitudes. Small-diameter shadow shields would provide essentially no protection for the sides of the cryogenic tank. The Sun side of large-diameter planetary shadow shields would be good reflectors of solar radiation. In fact, the effect of reflected solar flux incident on the tank end and side surfaces might even be larger than direct planetary flux on these tank surfaces.

The effectiveness of a simple system of double shadow shields (with diam. equal to the propellant-tank diam.) in reducing the hydrogen heat-absorption rate of the tank end due to planetary radiation is shown in figures 9(a) and (b). Again, the stage is assumed to be oriented with its longitudinal axis alined along the Sun-Earth line. In this position, solar flux is not directly incident upon either the tank sides or the tank end facing the planet. However, solar flux is reflected from the planet surface onto both the tank end and tank sides. The emissivity and absorptivity have been assumed equal to 0.1. Figure 9(a) shows the shadow-shield spacing ratio that minimizes the hydrogen heat-absorption rate against the ratio of altitude above the Earth's surface to the

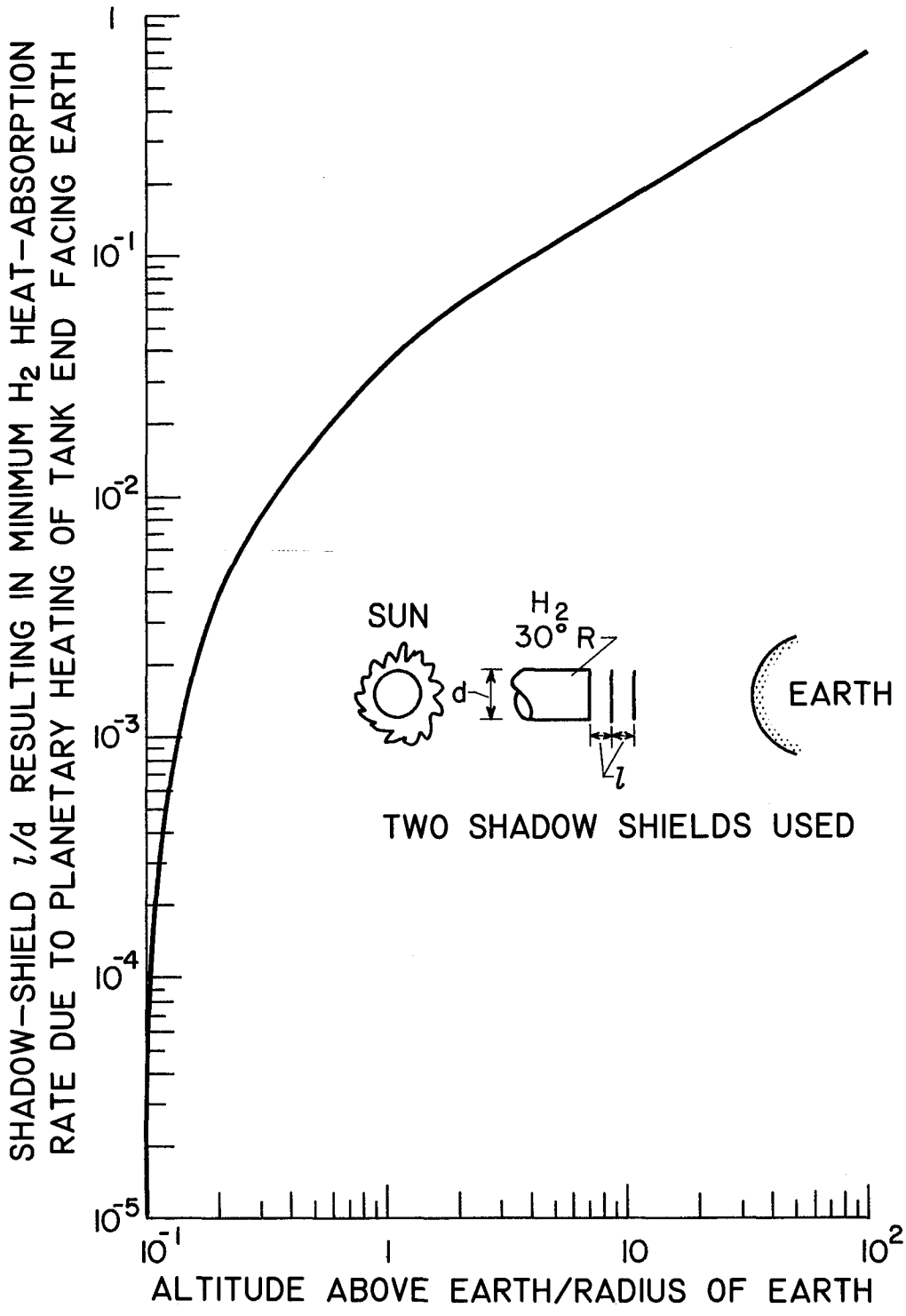

(a) Effect of altitude on optimum shield spacing.

Figure 9. - Double shadow shields for reducing heating effect of earth flux ($\alpha = \epsilon = 0.1$).

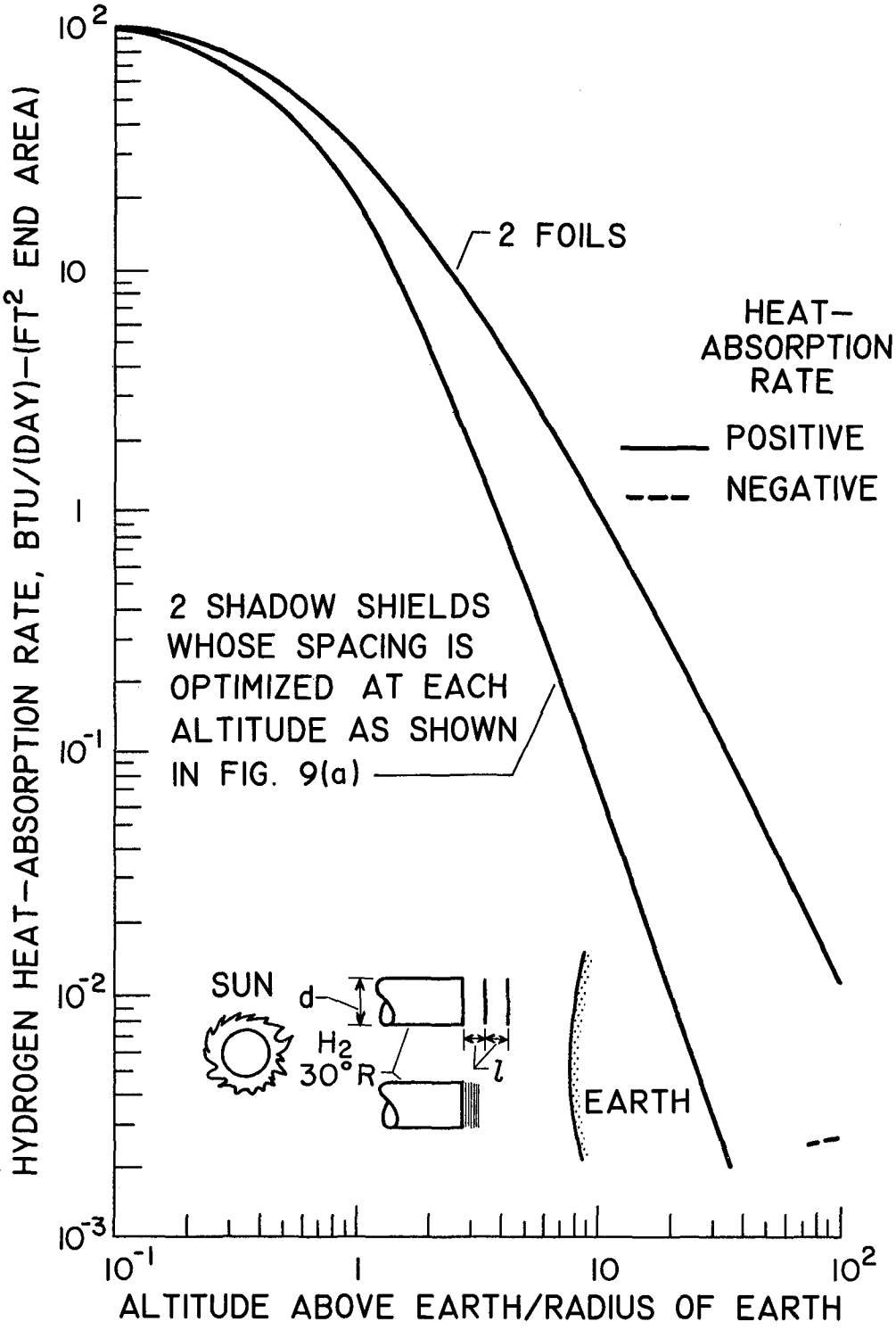

(b) Hydrogen heat-absorption rate corresponding to optimum shadow-shield spacing.

Figure 9. - Concluded. Double shadow shields for reducing heating effect of earth flux ($a = \epsilon = 0.1$).

Earth's radius. These spacing ratios decrease rapidly for decreasing abscissa values of less than 1. At a value of (altitude)/(planet radius) of 0.1, the heat-absorption rate is minimized with the small spacing ratio of about 10^{-5} (which corresponds to a spacing between 10-ft-diam. shields of 0.0012 in.). The heat-absorption rates that correspond to these spacing ratios are shown in figure 9(b). For reference, the upper curve shows the absorption rate for two closely spaced foils. As might be expected from the theory, the shadow-shield and foil curves approach each other when the optimum spacing between shadow shields is extremely small (at low altitudes).

In order to compare the magnitude of the heat-absorption problem in the vicinity of planets other than Earth, figure 10 is included. For this figure it was arbitrarily assumed that the spacing ratio l/d between adjacent shadow shields was 0.1 and that emissivity and absorptivity were also equal to 0.1. Heat transfer only on the end of the tank facing the planet was considered. The hydrogen heat-absorption rate is shown against the ratio of altitude above the planet surface to planet radius for Venus, Earth, and Mars. Venus, Earth, and Mars rank highest to lowest in that order comparing the heat-absorption rates at a constant value of the ratio of altitude to planet radius. For low altitude ratios, the absorption rates are on the order of 700 to 140 Btu per day per square foot of end area, which are prohibitively high for most applications.

FOILS. - The effectiveness of foil materials in reducing the hydrogen heat-absorption rate due to planetary heating can be substantial, as shown in figure 11. It was assumed for this figure that the absorption

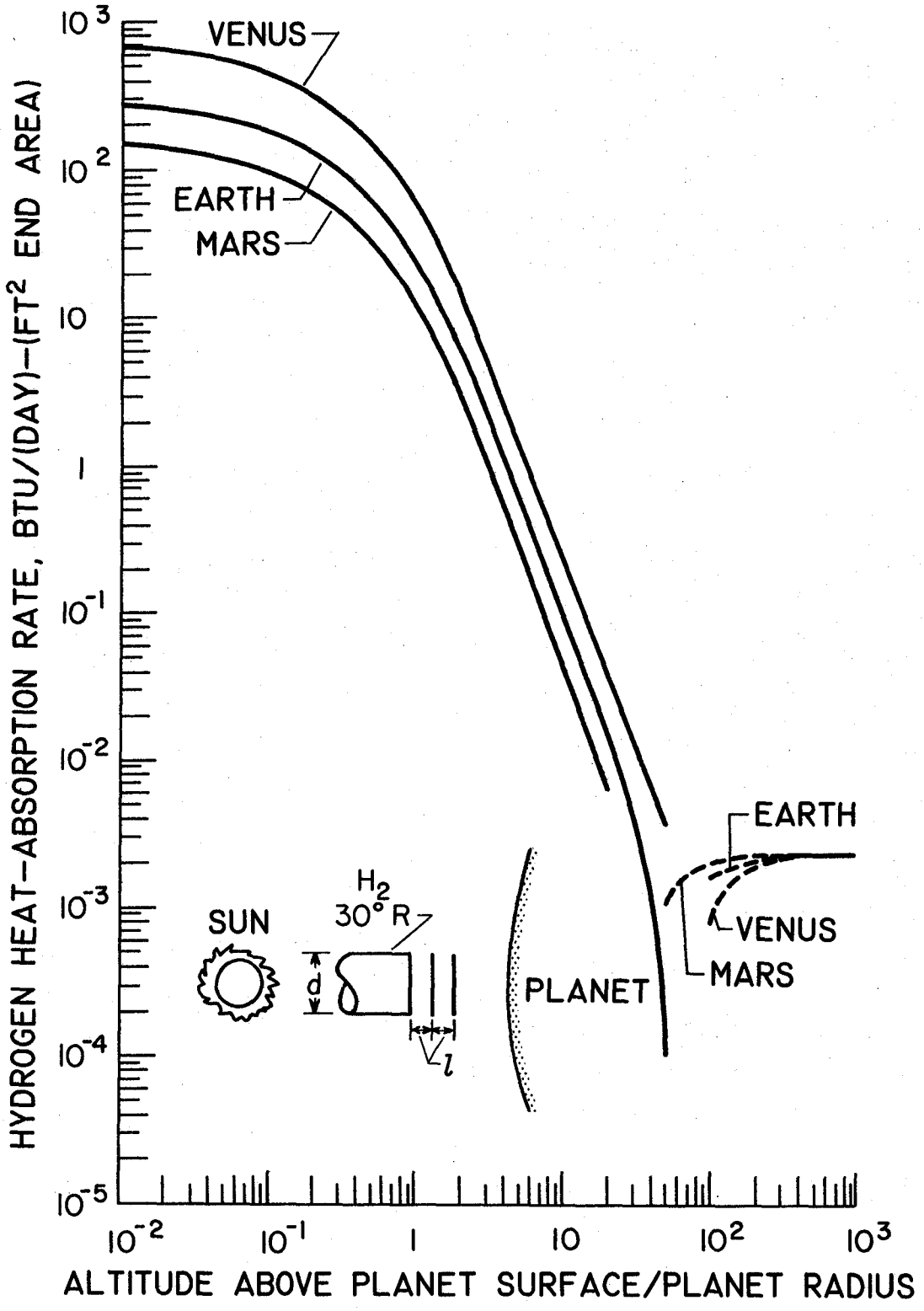

Figure 10. - Effect of altitude above several planets on hydrogen heat-absorption rate with double shadow shields ($\alpha = \epsilon = 0.1$, $l/d = 0.1$).

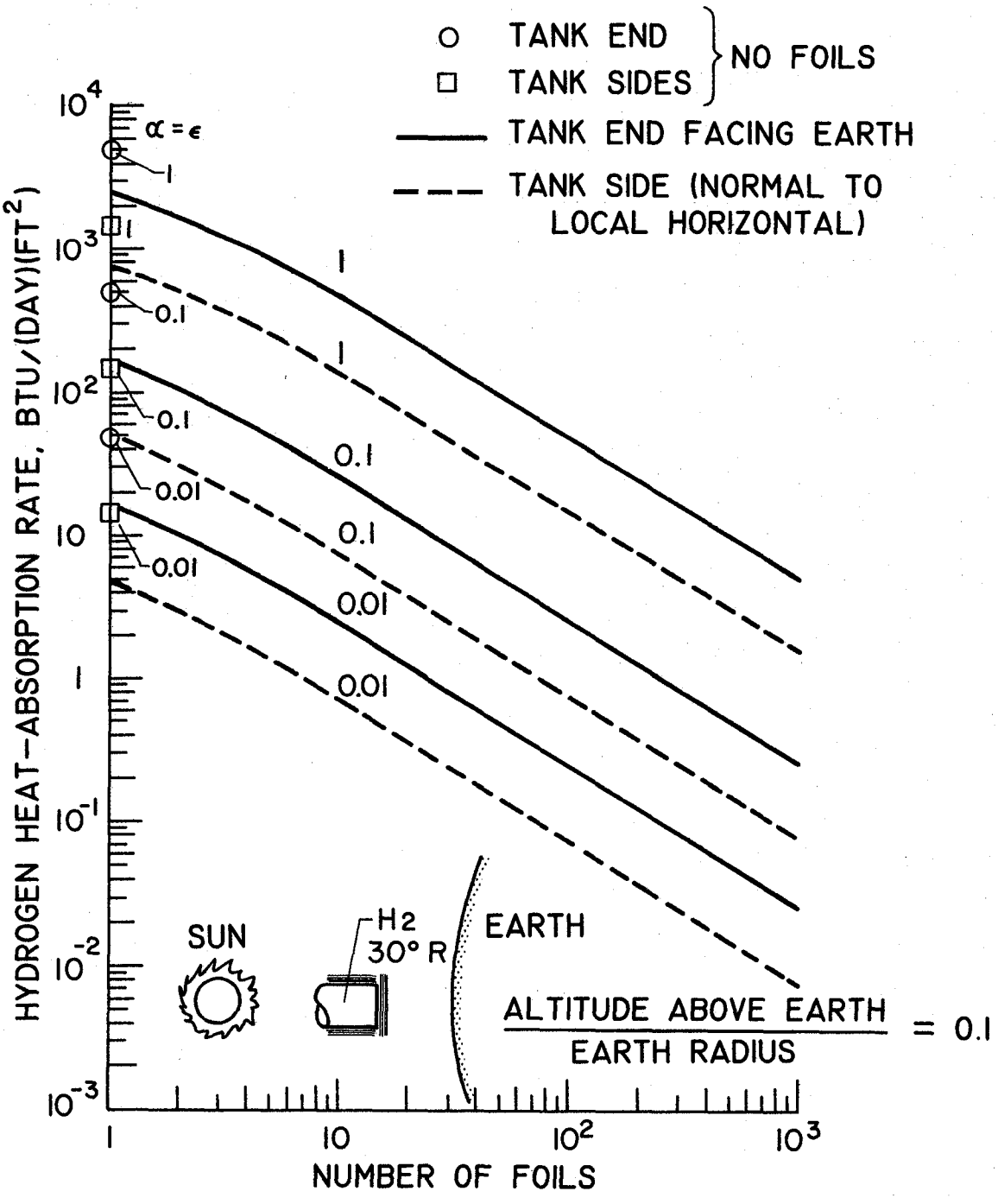

Figure 11. - Effect of number and emissivity of foils on hydrogen heat-absorption rate due to planetary flux.

rates are due only to the heat transfer through the surface specified and that the stage is alined on the Sun-Earth axis as in the sketch. Foils are assumed to cover completely the tank sides and tank end facing the Earth. Hydrogen heat-absorption rate is shown against the number of foils for emissivity = absorptivity = 1, 0.1, and 0.01. Also shown for reference are absorption rates with no foils on the tank. Either increasing the number of foils or decreasing the foil emissivity decreases the hydrogen heat-absorption rate. Absorption rates on the tank sides are less than those on the tank end, because the vertical angle factor is less than the horizontal angle factor for a particular altitude. However, foils would still be required on the tank sides to achieve low absorption rates.

TRAJECTORY VARIABLES. - Thus far, the methods of protecting a cryogenic-tank surface from external heating have included using shadow shields, foils, combinations of these, orientation, and special coating materials. One other factor that should be included here is trajectory considerations, since the total heat absorbed on any mission will be the integral of the heat-absorption rate with respect to time. These trajectory effects are considered in detail in reference 8.

As mentioned previously, the heat-absorption rate due to planetary heating is a strong function of the altitude above the planet. If small heat-absorption rates are desired while orbiting a planet, then the vehicle must operate at high altitudes. One means of having low-altitude capabilities and small heat-absorption rates is to utilize elliptic orbits. Here the high heat-absorption rates are encountered only for short

time periods, and thus the total heat absorbed per orbit will be much less than the heat absorbed for a low-altitude circular orbit.

Likewise, the escape and entry trajectories are also important in the overall storage problem. Vehicles with low thrust-to-weight ratios will absorb more heat (upon escaping or entering a planet orbit) than will vehicles with high thrust-to-weight ratios. However, as shown in reference 8, for thrust-to-weight ratios greater than about 0.01, escape and entry heat absorption is generally negligible. Most chemical and nuclear rockets have thrust-to-weight ratios greater than 0.1.

COMPARISON OF METHODS. - The effectiveness of the various thermal-protection techniques for reducing the rate of absorption of flux is shown in figure 12. The hydrogen heat-absorption rates for the end of a cryogenic tank protected by either shadow shields, or foils, or shadow shields with foils, are plotted against the ratio of altitude above the Earth to Earth radius. The absorptivity and emissivity were assumed equal to 0.1. It is apparent that widely spaced shadow shields are relatively ineffective at low altitudes. This conclusion was also reached in reference 21. At high altitudes, where the planet flux is more nearly parallel (and almost insignificant in magnitude), the shadow shields are more effective. Augmentation of these shadow shields with foils lowers the heat-absorption rate by a factor of about 10. However, at high altitudes, practically the same absorption rates can be obtained with foils alone. Thus, it appears that an attractive method of reducing the effect of planetary heating is to employ foils on all surfaces, since the additional advantage of using shadow shields is relatively small. Below altitudes of about 2.2 Earth radii, the ten foils are at

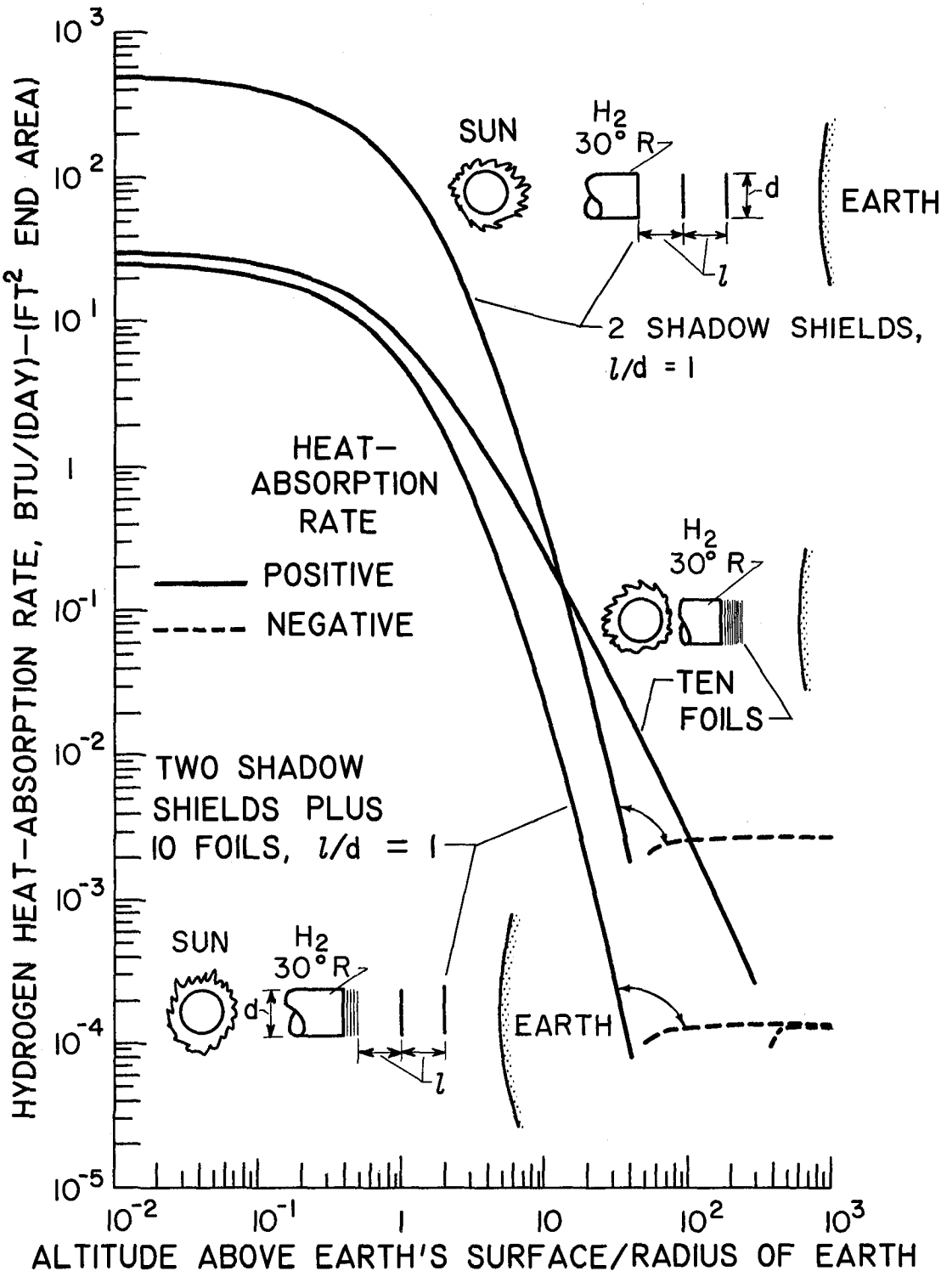

Figure 12. - Effectiveness of various devices for reducing effect of planetary flux ($\alpha = \epsilon = 0.1$).

least an order of magnitude more effective than two shadow shields. At 14 Earth radii, the two are equivalent. A possible disadvantage of planetary shadow shields is that they will require a continuous orientation toward the planet, thus allowing other unprotected cryogenic-tank surfaces to be exposed to direct solar flux.

DESIGN OF A THERMAL-PROTECTION SYSTEM FOR A MARS MISSION

Thus far, the methods of thermally protecting a cryogenic tank have been treated by considering an isolated portion of the tank subjected to a constant internal or external flux. The purpose of this section is to integrate these findings and demonstrate a method of minimizing the payload weight penalty of a complete protection system for a particular space vehicle and for a specific mission. All cryogenic-tank surfaces will be considered, and a variety of heating environments will prevail. The vehicle used will be a hydrogen-oxygen terminal stage. A terminal stage has been selected because it usually is exposed to the most severe heating environment.

OPTIMIZATION PROCEDURE. - If it is assumed that the payload weight of the terminal stage is to be maximized, a relation between payload weight, boiloff weight, and thermal-protection weight can be developed. The stage gross weight is

$$W_g = W_{pl} + W_{up} + W_{st} + W_{bo} + W_{tp} \tag{8}$$

where W_{bo} is the propellant vented overboard as a vapor due to heat absorption by the propellant tanks (not part of W_{up}). If the material used for thermal protection is not jettisoned before the propellants are burned, then

$$W_{up} = \left(1 - \frac{1}{e^{\Delta v/Ig}}\right)(W_g - W_{bo}) \tag{9}$$

The structure weight can be approximated as follows:

$$W_{st} = W_g\left[0.08\,\frac{(W_{up} + W_{bo})}{W_g} + 0.02\,\frac{F}{W_g}\right] \tag{10}$$

where $0.08(W_{up} + W_{bo})$ and $0.02F$ are representative values for the tankage structure weight and the thrust sensitive weight, respectively. If these expressions for propellant and structural weight are substituted in the original expression for gross weight, the resultant expression is

$$W_g = \frac{W_{pl} + W_{tp} + W_{bo}(1.08/e^{\Delta v/Ig})}{(1.08/e^{\Delta v/Ig}) - 0.08 - 0.02F/W_g} \tag{11}$$

or, in a more convenient form,

$$W_{pl} = W_g\left(\frac{1.08}{e^{\Delta v/Ig}} - 0.08 - 0.02\,\frac{F}{W_g}\right) - W_{tp} - W_{bo}\left(\frac{1.08}{e^{\Delta v/Ig}}\right) \tag{12}$$

where F/W_g is the thrust-to-gross-weight ratio. From this final expression for W_{pl}, it is apparent that, for fixed values of W_g, Δv, I, and F/W_g, the payload weight is

$$W_{pl} = \text{constant} - \left[W_{tp} + W_{bo}\left(\frac{1.08}{e^{\Delta v/Ig}}\right)\right] \tag{13}$$

Thus, in order to maximize the payload weight, it will be necessary to minimize the sum of the thermal-protection weight and $\left(\frac{1.08}{e^{\Delta v/Ig}}\right)$ times the boiloff weight.

ASSUMPTIONS. - The mission selected was a 378-day round trip to Mars, which included 20 days spent in a 1000-mile circular orbit about Mars. After the 20-day waiting period, the terminal-stage propellants were used to provide a 3.35-mile-per-second velocity increment (Δv) to the payload for the return trajectory to Earth. The initial

thrust-to-gross-weight ratio of the stage was 0.5, and the specific impulse of the propellants was 425 seconds. The hydrogen and oxygen were stored in 10-foot-diameter cylindrical tanks at 30° and 140° R, respectively. The hydrogen- and oxygen-tank lengths were 10 and 3.5 feet, respectively. Components of the stage were arranged in the order: payload, oxygen tank, hydrogen tank, and engine. By orienting the stage with the payload pointed at the Sun during all coast phases of the trip, the heating effect of direct solar flux was avoided. In optimizing the thermal-protection system for the trip, the following assumptions were made:

(1) The thermal-protection system had fixed elements (i.e., no variable-geometry devices were considered).

(2) To prevent freezing of the propellants, no net heat loss was allowed for either the hydrogen or oxygen for any part of the trip.

(3) If a choice existed, hydrogen boiloff was used instead of oxygen boiloff to conserve weight.

(4) For all surfaces, the emissivity and absorptivity were equal. Values were limited to the range 0.1 to 0.9.

(5) The installed weight of foils was 0.01 pound per square foot per foil. Foil supports weighed 0.03 pound per foil.

(6) The Mars parking orbit was circular at an altitude of 1000 statute miles and contained the Sun-Mars axis.

PERFORMANCE AND WEIGHT BALANCE OF RESULTANT VEHICLE. - The heat-absorption rates for the end of the hydrogen tank and the sides of the oxygen and hydrogen tanks, all protected by ten foils ($\alpha = \epsilon = 0.1$), are plotted in figure 13 against angular position of the stage with

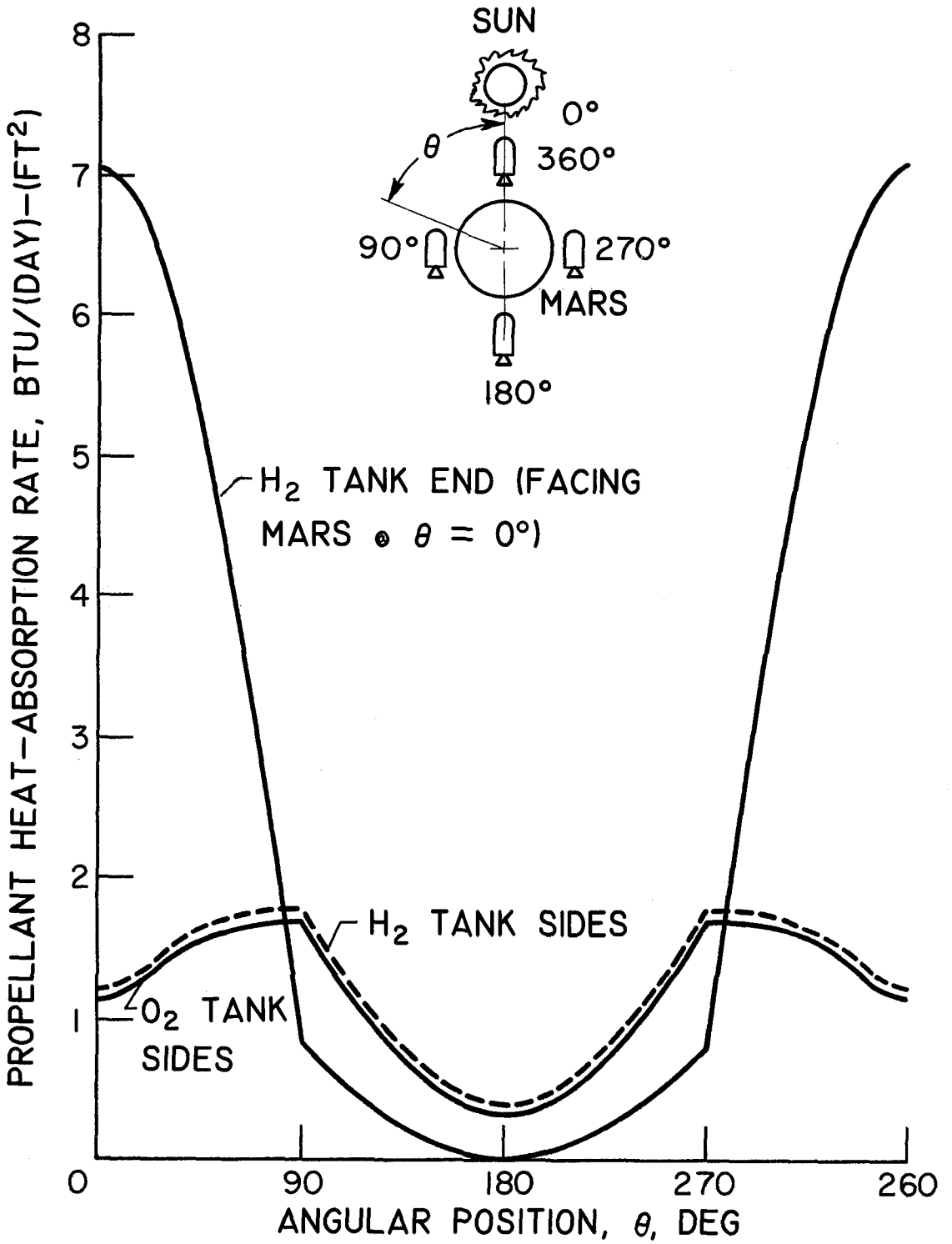

Figure 13. - Variation of heat-absorption rate with angular position for stage in circular orbit 1000 statute miles above Mars surface. Ten foils on H_2 and O_2 tank sides and on H_2 tank end ($\alpha = \epsilon = 0.1$).

respect to the Sun-Mars axis. Two factors that affect these curves profoundly are the variation of planetary flux with angular position around the planet and the variation of angle factors with angular position. The planetary flux varies with the temperature of the planet and also with the planet's albedo. Because the planet's temperature and albedo are not precisely known for various positions around the planet (and probably vary from day to day at a fixed position, anyway), the planetary flux cannot be predicted with great precision. Two positions where the flux and consequently the absorption rate may be easily estimated are the 0° (full daylight) and 180° (midnight) positions. For figure 13 the 90° and 270° values were obtained by taking the arithmetic mean value between those computed assuming a fully sunlit planet and a fully darkened planet. The flux between these points was assumed to vary according to a sine relation, the result of which is shown in figure 13.

By integrating the curves of figure 13, the average heat-absorption rates for a complete orbit were obtained. However, there is no reason to believe that the arbitrarily assumed number of foils (10) was also the optimum number of foils. This presents no particular difficulty in the optimization process, because from the ANALYSIS it can be seen that, if we assume that $\alpha_S = \epsilon_o = \epsilon_x = \epsilon_y$, then the absorption rate on these surfaces must be proportional to $\frac{\epsilon}{N(2 - \epsilon) + 1}$. Therefore, the propellant boiloff for a particular surface is a function of only one unknown, N, the number of foils on this surface. All other parameters affecting the boiloff are known from previous assumptions. Similarly, the weight of the thermal-protection system for a particular surface can be expressed in terms of the single unknown N. Then the optimum value of N

for each particular surface, shown in figure 14, is that value which minimizes the sum of $\left[W_{tp} + W_{bo}\left(\frac{1.08}{e^{\Delta v/Ig}}\right)\right]$.

By using this procedure it was possible to minimize the total payload weight penalty. The results of this optimization process are shown in sketch (b) of the terminal stage:

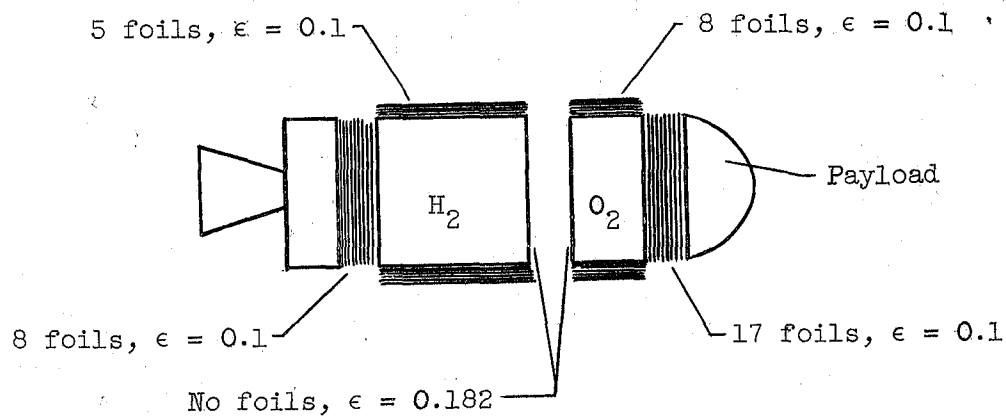

(b)

The number and emissivity of the foil surfaces are indicated. A higher value of emissivity between the oxygen and hydrogen tanks would have resulted in freezing of the oxygen during the 179-day coast from Earth to Mars. The foils and their supports weigh 110 pounds. During the 179-day phase of the trip, 99 pounds of hydrogen and no oxygen are vaporized and vented. During the 20 days in the Mars orbit, 114 pounds of hydrogen and 34 pounds of oxygen are vaporized and vented. The total propellant boiloff is therefore 247 pounds, and the payload weight penalty, $\frac{100\%}{W_{pl}}\left[W_{tp} + \left(\frac{1.08}{e^{\Delta v/Ig}}\right)W_{bo}\right]$, is only about 3 percent. Other weights are;

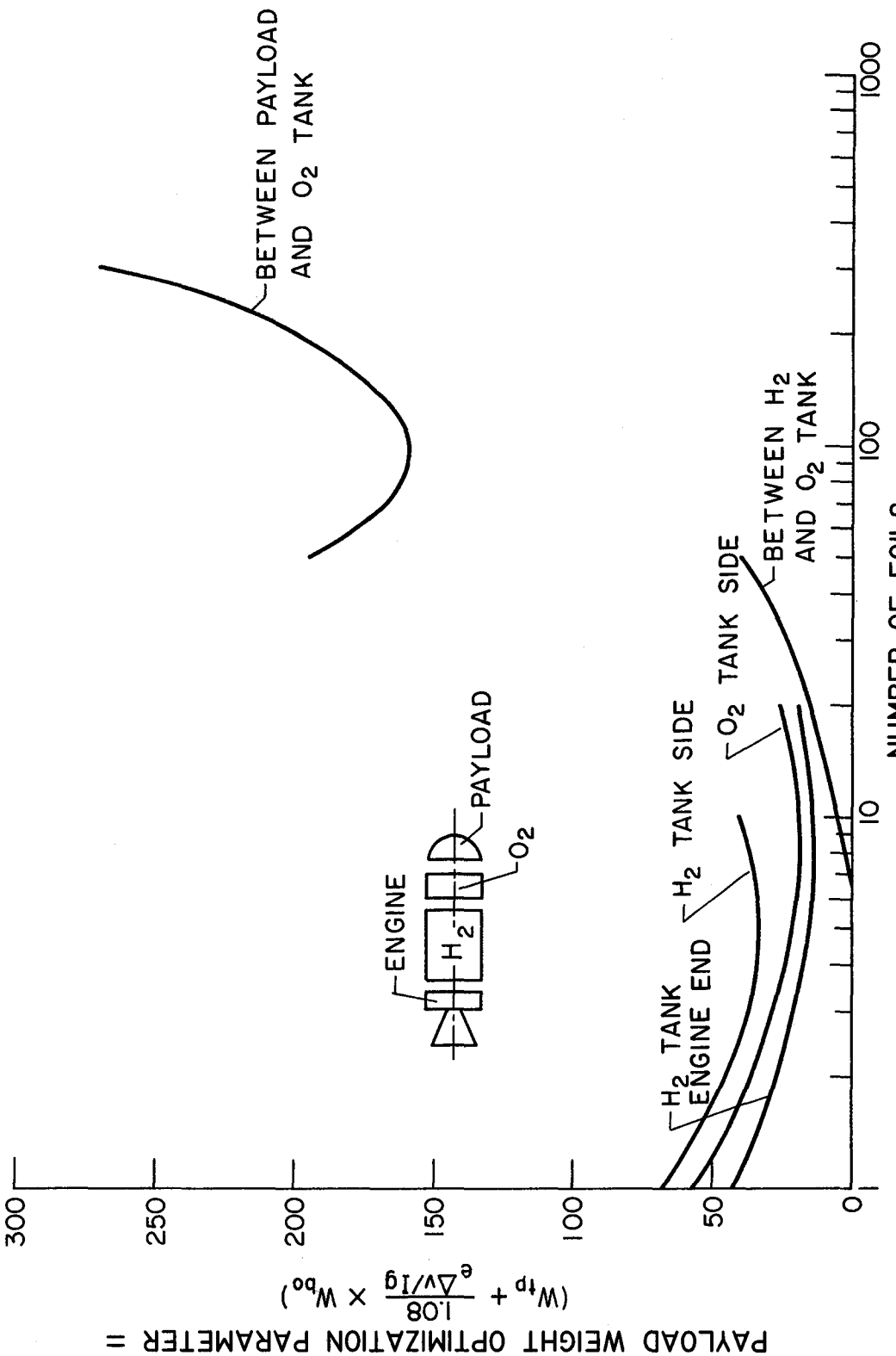

Figure 14. - Effect of variations in number of foils on payload weight optimization parameter. Stage in orbit 1000 statute miles above Mars for 20 days ($\alpha = \epsilon = 0.1$).

net payload, 6110 pounds; gross, 30,520 pounds; structure, 2083 pounds; and propellants, 21,970 pounds.

CONCLUDING REMARKS

The analytical techniques developed in this paper provide the basic information required to design thermal-protection systems for propellant tanks subjected to the thermal-radiation environment of space. The application of these theoretical relations has been demonstrated for cryogenic-propellant tanks. However, the methods used herein are equally applicable whether cryogenic or noncryogenic propellants are considered.

Shadow shields and foils can greatly reduce the heating of propellants due to both internal and external thermal radiation. For low-altitude planetary orbits, foils appear to be desirable for all cryogenic-tank surfaces exposed to planetary or solar radiation.

Thermal-protection systems have been discussed in detail. The optimum method of providing thermal protection for cryogenic propellants is strongly dependent upon the magnitude and duration of the thermal environment encountered during the mission.

It is recognized that several other factors may have an important effect on the choice of a thermal-protection system. These factors include aerodynamic heating during the boost trajectory, weightless-fluid dynamic phenomena, meteoroid penetrations (refs. 22 and 23), effect of meteoroids on reflective surfaces (ref. 24), materials problems (ref. 25), and nuclear-radiation heating (refs. 11 and 12).

There appears to be a need for further evaluation of multilayer shielding materials installed on propellant tanks. In particular, the effects of compressive loads and structural supports should be determined.

APPENDIX - SYMBOLS

A	cross-sectional area, sq ft
a	albedo = 1 - emissivity = reflectivity
d	diameter, ft
F	thrust, lb
$f_{1,2}$	angle factor (from refs. 8,10,28, and 29), fraction of total radiation leaving surface 1 that arrives at surface 2
g	acceleration due to gravity at Earth's surface, ft/sec^2
I	specific impulse, sec
k	apparent mean thermal conductivity of insulation, $(Btu)(ft)/(hr)(ft^2)(^oR)$
l	distance between radiation shields, ft
N	number of radiation shields
$\dot{Q}$	heat-transfer rate, Btu/hr
$(\dot{Q}/A)_y$	net rate of heat absorption by surface y, Btu/(hr)(sq ft)
r	radius, ft
S	distance from center of Sun, astronomical units
T	temperature, ^oR
t	thickness of insulation, ft
W	weight, lb
Y	external heat flux incident on bare tank or tank-protection system, Btu/(hr)(sq ft)
y	any surface or tank surface
z	= 1 on Sun side of planet, = 0 on dark side of planet
α	total hemispherical absorptivity
α_S	total hemispherical absorptivity for solar flux
α_Y	total hemispherical absorptivity for flux Y

ϵ	total hemispherical emissivity
ϵ_o	total hemispherical emissivity of outermost surface at surface temperature
Δv	stage velocity increment, ft/sec
ρ	density, lb/cu ft
σ	Stefan-Boltzmann constant, $Btu/(hr)(ft^2)(^oR^4)$

Subscripts:

B	all surfaces facing inward to propellant tank
bo	boiloff
F	all surfaces facing outward from propellant tank
g	gross
o	reflective surface upon which external radiation is incident
P	relative to planet
pl	payload
S	Sun or solar
st	structure
tp	thermal protection
up	useful propellant
x	adjacent tank
y	tank for which heat-absorption calculations are being made

REFERENCES

1. Kramer, J. L., Lowell, H. H., and Roudebush, W. H.: Numerical Computations of Aerodynamic Heating of Liquid Propellants. NASA TN D-273, 1960.

2. Gray, V. H., Gelder, T. F., Cochran, R. P., and Goodykoontz, J. H.: External Bonded and Sealed Insulations For Liquid Hydrogen Fueled Rocket Tanks During Atmospheric Flight. NASA TN D-476, 1960.

3. Burry, R. V.: Liquid Propellant Storage In Earth Satellite Orbits. (Paper presented at April 7, 1960 session of Institute of Environmental Sciences, Los Angeles, California.)

4. Cramer, K. R.: Orbital Storage of Cryogenic Fluids. WADC Technical Note 58-282, October, 1958.

5. Burry, R. V., and Degner, V. R.: Liquid-Propellant Storage Evaluation For Space Vehicles. (Paper presented at 4th Symposium On Ballistic Missiles and Space Technology, UCLA, August, 1959.)

6. Love, C. C., Jr.: Liquid Hydrogen Transport Time Limits In Space. SAE Paper No. 1087-60, April, 1960.

7. Ehricke, Krafft A.: A Systems Analysis Of Fast Manned Flights To Venus and Mars. Part II: Storage of Liquid and Solid Hydrogen On Nuclear Powered Interplanetary Vehicles. ASME Paper No. 60-AV-1, June, 1960.

8. Smolak, G. R., and Knoll, R. H.: Cryogenic Propellant Storage For Round Trips To Mars and Venus. IAS Paper No. 60-23, 1960.

9. Himmel, S. C., Dugan, J. F., Jr., Luidens, R. W., and Weber, R. J.: A Study Of Manned Nuclear-Rocket Missions to Mars. IAS Paper No. 61-49, Jan., 1961.

10. Smolak, G. R., Knoll, R. H., and Wallner, L. E.: Analysis Of Thermal-Protection Systems For Space-Vehicle Cryogenic-Propellant Tanks. NASA TR (in the publication process).

11. Brun, R. J., Livingood, J. N. B., Rosenberg, E. G., and Drier, D. W.: Analysis of Liquid-Hydrogen Storage Problems For Unmanned Nuclear-Powered Mars Vehicles. NASA TN D-587, 1961.

12. Trapp, R. F., and Wilson, J. H.: Optimizing Reactor Shield Propellant Boiloff and Tank Pressure. Douglas Aircraft Company, Inc. Engineering Paper number 1140.

13. Scott, R. B.: Cryogenic Engineering. D. Van Nostrand Company, Inc. Princeton, New Jersey.

14. Gaumer, R. E., Clauss, F. J., Sibert, M. E., and Shaw, C. C.: Materials Effects In Spacecraft Thermal Control. Lockheed Missiles and Space Division LMSD-704019, November, 1960.

15. Gaumer, R. E.: Determination Of The Effects Of Satellite Environment On The Thermal Radiation Characteristics Of Surfaces. SAE Paper Number 339C, April, 1961.

16. Schocken, K.: Spectral Emissivities and Solar Absorptivities. ABMA Report Number DV-TN-72-58, September 1, 1958.

17. Riede, P. M., and Wang, D.I-J.: Characteristics and Applications Of Some Superinsulations. 1959 Cryogenic Engineering Conference.

18. Hnilicka, M. P.: Engineering Aspects Of Heat Transfer In Multilayer Reflective Insulation and Performance Of NRC Insulation. 1959 Cryogenic Engineering Conference.

19. Kropschot, R. H., Schrodt, J. E., Fulk, M. M., and Hunter, B. J.: Multiple Layer Insulation. 1959 Cryogenic Engineering Conference.

20. Olson, O. H., Morris, J. C., Betz, H. T., and Schwin, B. D.: Determination Of Emissivity and Reflectivity Data On Aircraft Structural Materials, Part I (1958), Part II (October 1958), Part II Supplement (October 1958) and Part III (January 1959). WADC Technical Report 56-222, Armour Research Foundation.

21. Olivier, J. R., and Dempster, W. E.: Orbital Storage of Liquid Hydrogen. NASA MTP-M-LOD-DL-3-61, Feb. 16, 1961.

22. Bjork, R. L.: Meteoroids Versus Space Vehicles. ARS Paper Number 1200-60. May 1960.

23. Wallace, R. R., Vinson, J. R., and Kornhauser, M.: Effects Of Hypervelocity Particles On Shielded Structures. American Rocket Society Paper No. 1683-61, April 4-6, 1961.

24. Henderson, R. E., and Stanley, P.: The Effect Of Micrometeorites On Reflecting Surfaces. Institute of Environmental Sciences. April 6, 1960.

25. Lad, R. A.: Survey Of Materials Problems Resulting From Low-Pressure and Radiation Environment In Space. NASA TN D-477, November, 1960.

26. Bailey, B. M., et al: Storage, Transfer, and Servicing Equipment For Liquid Hydrogen. WADC Technical Report 59-386, July, 1959.

27. Black, I. A., Fowle, A. A., and Glaser, P. E.: Development Of High-Efficiency Insulation. 1959 Cryogenic Engineering Conference.

28. Leuenberger, H., and Person, R. A.: Compilation Of Radiation Shape Factors For Cylindrical Assemblies. ASME Paper Number 56-A-144, 1956.

29. Ballinger, J. C., Elizalde, J. C., and Christensen, E. H.: Thermal Environment Of Interplanetary Space. SAE Paper Number 344B, 1961.